

PhD Thesis

**INVESTIGATIONS OF CERTAIN ORGAN SPECIFIC TOXIC EFFECTS OF TITANIUM
DIOXIDE NANOPARTICLES BY *IN VIVO* AND *IN VITRO* METHODS**

Tamara Horváth

**Supervisors: Tünde Vezér MD PhD
 András Papp PhD**

**Department of Public Health
University of Szeged
Szeged
2019**

The Applicant's Relevant Publications

- I. Horváth T, Papp A, Kiricsi M, Igaz N, Trenka V, Kozma G, Tiszlavicz L, Rázga Zs, Vezér T: Titán-dioxid-nanopálcikák tüdőre kifejtett hatásának állatkísérletes vizsgálata szubakut patkány modellben.
Orvosi Hetilap 160: 57–66 (2019). IF₂₀₁₈=0.322
- II. Horváth T, Papp A, Igaz N, Kovács D, Kozma G, Trenka V, Tiszlavicz L, Rázga Z, Kónya Z, Kiricsi M, Vezér T: Pulmonary impact of titanium dioxide nanorods: examination of nanorod-exposed rat lungs and human alveolar cells.
International Journal of Nanomedicine 13:7061-7077 (2018). IF₂₀₁₈=4.370
- III. Horváth T, Vezér T, Kozma G, Papp A: Functional neurotoxicity and tissue metal levels in rats exposed subacutely to titanium dioxide nanoparticles via the airways.
Ideggyógyászati Szemle / Clinical Neuroscience 71:35-42 (2018). IF₂₀₁₈=0.252
- IV. Horváth T, Papp A, Kovács D, Kálomista I, Kozma G, Vezér T: Electrophysiological alterations and general toxic signs obtained by subacute administration of titanium dioxide nanoparticles to the airways of rats.
Ideggyógyászati Szemle / Clinical Neuroscience 70:127-135 (2017). IF₂₀₁₇=0.322
- V. Horváth T, Szabó A, Lukács A, Oszlánzi G, Kozma G, Kovács D, Kálomista I, Vezér T, Papp A: Titán-dioxid nanorészecskék szubakut neurotoxicitásának vizsgálata patkány modellben.
Egészségtudomány 60: 7-23 (2016).
- VI. Horváth T, Vezér T, Papp A: Possible Neurotoxicity of Titanium Dioxide Nanoparticles in a Subacute Rat Model.
In: Proceedings of the 21st International Symposium on Analytical and Environmental Problems (Alapi T, Ilisz I, eds.; ISBN 978-963-306-411-5). pp. 368-372 (2015).

Abstracts

1. Horváth T, Papp A, Kozma G, Kiricsi M, Igaz N, Kálomista I, Vezér T: General and nervous system toxicity of titanium dioxide nanoparticles investigated by in vivo and in vitro methods.
NKE XI. Konferenciája "Krónikus betegségek megelőzése". Szeged; 2017.08.30 - 09.01.
Népegészségügy 95:160-161. (2017)
2. Horváth T, Kozma G, Kovács D, Kálomista I, Vezér T, Papp A: Funkcionális idegrendszeri változások vizsgálata titán-dioxid nanorészecskékkel kezelt patkányokban.
Magyar Élettani, Klinikai és Kísérletes Farmakológiai, Mikrocirkulációs és Vaszkuláris Biológia Társaságok Közös Tudományos Konferenciája, Debrecen, 2017.06. 13. - 06.16.
Absztrakt P 1.1.8., pp.9-10.

3. Horváth T, Kozma G, Igaz N, Kálomista I, Vezér T, Papp A: Detection of neurotoxicity of titanium dioxide nanoparticles in vivo and in vitro measurements.
19th Danube-Kris-Mures-Tisa (DKMT) Euroregional Conference on Environment and Health, Szeged, 2017.06.09. - 06.10.
Program and Abstracts (Paulik E, ed.; ISBN 978-963-306-535-8) p. 43.
4. Horváth T: A titán-dioxid toxicitásának lehetősége szubakut patkánymodellben.
FAMÉ 2016: Magyar Farmakológiai, Anatómus, Mikrocirkulációs és Élettani Társaságok Közös Tudományos Konferenciája, Pécs, 2016.06.01. - 06.04.
Program P 1.1.8; p.28.
5. Papp A, Horváth T, Paulik E, Nagymajtényi L, Vezér T: Titanium dioxide nanoparticles: applications, environmental presence, and health risk.
18th Danube-Kris-Mures-Tisa (DKMT) Euroregional Conference on Environment and Health, Újvidék, 2016.06.02. - 06.04.
Book of Abstracts (Škrbić B, ed.; ISBN 978-86-6253-059-2), p. 22.
6. Horváth T, Horváth E, Oszlanczi G, Kozma G, Kovács D, Kálomista I, Vezér T, Papp A: Titán-dioxid intratracheális expozícióval összefüggő neurotoxicitás vizsgálata patkány modellben.
XII. Fiatal Higiénikusok Fóruma, Hajdúszoboszló, Debrecen, 2016.05.18. - 05.20,
Programfüzet, p. 14.
7. Horváth T, Horváth E, Máté Zs, Szabó A, Lukács A, Oszlanczi G, Vezér T, Papp A, Kozma G, Kovács D, Kálomista I: Detection of Neurotoxicity of Titanium Dioxide nanoparticles in a Subacute Rat Model.
IBRO Workshop 2016. Budapest, 2016.01.21.- 01.22.
Program and Abstracts p. 247-248.

SUMMARY

The world of nanoparticles (NPs: particles with not more than 100 nm typical diameter at least in one dimension) has gained a great deal of attention in the last ca. 30 years in various fields of research, including life and health sciences. NPs can be cubical or spherical grains, but elongated structures: nano-rods, -wires, -tubes etc. also exist.

This size lends some peculiar characteristics to the NPs, so properties and behavior of the same chemical substance in nano vs. more conventional states can be different. This is due to the high surface-to-volume ratio and to surface reactivity, and leads to biological, including toxicological, interactions not seen with traditional materials, resulting possibly in novel health risks. The relationship between elevated level of ambient airborne NPs and human morbidity and mortality has been generally accepted by now, and particulate air pollution has been recognized as an environmental carcinogenic agent.

Among man-made NPs, by-products of various technological procedures, acting as pollutants, and purposefully produced nanomaterials are to be distinguished. Engineered nanomaterials are becoming part of everyday life, in form of NP-containing consumers' products. The broad spectrum of application with concomitant human exposure raises the question of health risk. Here, a major problem is the lack of toxicity data for most manufactured NPs – and this is why nanotoxicology, an interdisciplinary field related to both environmental hygiene and nanotechnology, emerged.

In case of exposure by NPs, the most likely entrance in the (human or animal) organism is, first of all for pollutants, but partly also for nanotechnological NPs, inhalation of air containing a nano-aerosol. NPs, deposited either in the nasopharynx or in the alveoli, are not held back by barriers like the alveolar and capillary wall, and reach other target organs by being phagocytosed and transferred along the lymphatic system, or by different mechanisms including transcytosis, and finally are distributed throughout the body via the circulation. In case of consumers' products, gastrointestinal and dermal uptake may also be of interest.

In the aqueous microenvironment of living tissues, surface reactivity of NPs leads to generation of reactive oxygen species (ROS). The resulting oxidative stress can induce damage to biomolecules, primarily lipids and proteins, and finally induce inflammation and/or cytotoxicity.

Titanium dioxide (TiO₂) is a white, odorless, water insoluble soluble solid of high chemical stability and high melting temperature. Its major crystal forms are anatase and rutile. TiO₂ as

white pigment is used also in the food and pharmaceutical industry. TiO₂ NPs of various shapes (grains, rods, wires, tubes) have a broad range of application.

Human exposure to TiO₂ NPs may occur during manufacturing, processing, and use; in form of aerosols, suspensions or emulsions. The most health relevant routes of exposure in workplaces are inhalation and dermal exposure, while non-occupational exposure is most likely dermal or oral. Ill effects – increased oxidative stress, inflammation, lung damage – due to airborne TiO₂ in humans suffering occupational exposure have been in fact documented and successfully modeled in animals. Nervous system effects would also be expected for an agent able to cross the blood-brain barrier and to cause oxidative stress. However, human data to this point are scarce. Animal experiments, done predominantly in mice and less in rats, showed various central nervous alterations including cell damage, altered synaptic transmission and plasticity, memory impairment and increased anxiety. Other organs, including the kidneys, also showed signs of damage – activation of inflammatory mediators, histological damage, decreased function – in rats and mice on TiO₂ NP administration. These effects could be deduced to cellular uptake of nano-TiO₂, followed by ROS generation, engulfment by lysosomes, and release of enzymes from the latter initiating inflammation and cell death.

Exposure of humans to TiO₂ NPs can take place both in occupational settings, in the residential environment, or during free-time activities, and certain properties of the TiO₂ NPs suggest harmful effects on various organs and organ systems of humans or animals but the available reports on such effects are not yet conclusive. Based on the experience gained at the Department of Public Health in examining the toxicity of metal oxide NPs for over 10 years, and on the properties and possible effects of TiO₂ NPs outlined above, it was decided to investigate in the present PhD work the alterations evoked by TiO₂ NPs with a complex approach. By treating rats subacutely via the airways, and applying pathomorphological, chemical, biochemical as well as behavioral and electrophysiological methods, answer to the following questions was sought:

- Is it possible to create effective internal TiO₂ NP load in the treated rats by intratracheal instillation?
- Do the TiO₂ NPs cross biological barriers, reach the circulation and/or distant organs (including essential targets such as brain, liver, kidneys), and show deposition in the latter?
- What alterations – morphological and/or biochemical-molecular – are elicited in the gate organ, the lungs?

- Is the set of behavioral and electrophysiological methods, applied previously to study the effects of other metal oxide NPs, suitable to examine the neurotoxic effects of TiO₂ NPs?
- What are the main functional alterations detectable at the level of cognitive behavioral and electrophysiological phenomena?
- How are the kidneys, as possible organs of excretion, affected by the internal TiO₂ NP load?
- What is the relationship between the observed morphological (cellular or subcellular), as well as biochemical and neuro-functional, alterations and Ti or TiO₂ NP load detected in the corresponding organs?
- What implications have the results, presented in this thesis, to human, primarily occupational, health risk?

Rod-shaped TiO₂ NPs of 15x65 nm size were suspended in phosphate-buffered saline containing 1% polyacrylic acid. For *in vivo* experimentation, the NPs were given to young adult male Wistar rats by intratracheal instillation for altogether 28 days in a 5 treatment days per week scheme, in 5 (low dose, *LD*), 10 (medium dose, *MD*), and 18 (high dose, *HD*) mg/kg b.w. dose. There was an untreated control (*C*) and a vehicle control (*VC*) group also. The behavioral examinations applied were climb test, elevated plus maze, open field, as well as acoustic startle response and pre-pulse inhibition. In electrophysiology, cortical spontaneous and evoked activity, and peripheral nerve action potential were recorded and analyzed. Pathomorphological analysis was done by light and electron microscopy on lung and kidney tissue sections. Ti levels were determined in blood, brain, lung and kidney samples; oxidative stress markers in brain and lung; and cytokines in lung samples. The doses, and the majority of methods, were based on a previous pilot study. In the *in vitro* work, A549 cells (of human alveolar origin) were exposed by the TiO₂ nanosuspension, and cell viability and ROS generation was measured.

Depending on the normality of data distribution, checked by Shapiro-Wilk test, body/organ weights, as well as behavioral and histopathological data, were analyzed by one-way ANOVA and post hoc Tukey test, while for electrophysiological and chemical-biochemical data nonparametric Kruskal-Wallis ANOVA and post hoc Mann-Whitney U-test was used. Changes of the open field activity, recorded three times during the experimental period, were tested by repeated measures ANOVA and post hoc Tukey test. The limit of significance was $p < 0.05$ for all measurements. The subacute nano-TiO₂ exposure had no effect on body weight but the body weight-related relative weight of the lungs and kidneys increased significantly in the *HD* group vs. *C* and *VC*.

VII

Measured Ti content of the *HD* treated rats' lungs increased massively, and presence of TiO₂ NPs was verified by light and electron microscopy. This was accompanied by increase of oxidative stress indicators and inflammatory cytokines. In the *in vitro* test, cells showed dose- and time dependent viability decrease and ROS increase. NPs were seen in and on the exposed cells, and presence of Ti was directly verified by energy-dispersive X-ray spectroscopy.

The treated rats' behavior indicated increased anxiety. They spent more time in the corner zones of the open field box, and tended to avoid open arms of the elevated plus maze. This open field behavior developed in a time- and dose-dependent manner. Their acoustic startle response showed delayed reaction. Besides, the treated rats appeared to have impaired muscle force or motor coordination in the climb test.

The general trend of the electrophysiological results showed delayed and increasingly fatigable evoked activity, both cortical and peripheral. The tested corticostriatal connection was also weaker. In several of the electrophysiological and behavioral parameters, the change was in fair correlation with the measured Ti level of the corresponding brain parts.

The Ti content in the kidneys was significantly elevated in the treated vs. control rats but the increase was not fully proportional to the dose. By light microscopy, necrotic glomerular and tubular epithelial cells were seen in the kidney sections of *MD* and *HD* treated rats, together with dark, dense objects – possibly aggregates of NPs phagocytosed by the tubular epithelial cells. TEM images also showed NPs and their intracellular aggregates.

The real determinant of a toxic effect is internal dose at the site or sites of action. In the present work, the highest levels of chemically detected Ti and visualized TiO₂ NPs were found in the lungs, but elevated Ti levels were found also in samples of blood as well as of organs including brain and kidneys. Translocation of NPs by means of phagosomes contained in alveolar macrophages was verified, and presence of NPs in the kidneys was also shown. This, together with detected Ti levels, outlined the complete fate of TiO₂ NPs and their metal content from uptake through sites of action up to excretion.

TiO₂ NPs could cause the observed functional alterations in the nervous system by several mechanisms. Oxidative stress, to which the nervous system is sensitive, may have played a major role. Increased lipid peroxidation could be measured in both brain and lung samples of the treated rats. Oxidative damage to membrane lipids is likely to result in changes of membrane fluidity and this way in alterations of membrane-bound events of pulse propagation and synaptic transmission. The chain of causal relationships from Ti levels in organs through oxidative stress up to functional alteration was supported by the correlations observed between

VIII

electrophysiological and behavioral signs of functional damage, and the level of Ti and TBARS in the brain.

Oxidative damage to mitochondria and energy shortage could affect ion pumps and transmitter turnover. Excess glutamate and abnormal ion gradients lead to disturbed synaptic transmission and spike propagation. Dysfunction of the dopaminergic neurons, especially sensitive to oxidative stress, might be responsible for the observed alterations of cognitive behavior. Beside dopaminergic hypofunction, excess glutamate also might have contributed to elevated anxiety. One further consequence of oxidative stress caused by TiO₂ NPs is inflammation. In our work, inflammation markers were detected in the exposed rats' lungs. From the lysosomes of macrophages, unable to break down the phagocytosed NPs, enzymes are released that initiate the cascade of cytokine activation. Some of the detected mediators suggested that inflammation, developing first in the directly affected lungs, was becoming systemic; including neuroinflammation and kidney damage.

Conclusion: Nanoparticulate forms of TiO₂, including non-spherical shapes, are used in numerous applications, and can cause human exposure from several, purposeful or accidental, sources. The physicochemical properties of TiO₂ NPs suggest health damaging effects via several possible mechanisms. Experimental results of the PhD work, described and discussed in this thesis, showed that the rod-shaped TiO₂ NPs with anatase crystal structure, when applied to the airways, remained partly in the lungs but partly caused systemic exposure and reached distant organs like the CNS and the kidneys. Damages caused by the NPs were observed in the lungs, kidneys and the nervous system, with oxidative stress as most likely common element. Up to now, such effects were documented in the literature mostly for spherical TiO₂ NPs. The damages observed in our experimental work, especially those in the nervous system, point to the human health relevance of such studies.

Based on the results presented in this thesis, the points of aims, listed above, can be answered as follows:

- By intratracheal instillation of suspended TiO₂ nanorods, effective internal load could be achieved.
- TiO₂ nanorods and/or their metal content were detected in samples of the lungs, CNS, and kidneys – indicating that the NPs crossed biological barriers, and outlining their complete fate from uptake through sites of action up to excretion.
- In the lungs, significant deposition of nano-TiO₂ and signs of oxidative stress were observed. Cytokine activation indicated acute and chronic inflammation.

- It was possible to detect and quantify neuro-functional alterations in the treated rats by the behavioral and electrophysiological methods applied.
- The behavioral alterations in the rats treated with TiO₂ nanorods were mostly related to increased anxiety, suggesting damage to the dopaminergic, and partly glutamatergic, regulation. Changes in the cortical evoked response underlined glutamatergic damage.
- In the treated rats' kidneys, elevated Ti levels were measured. Presence of NPs, and tissue alterations suggesting functional damage were observed.
- In several cases we could demonstrate that the alterations were proportional to the locally determined Ti load.
- Regarding mass production and widespread application of nano-TiO₂, including nanorods, the results presented in this thesis have human health relevance, first of all for those suffering occupational exposure.

TABLE OF CONTENTS

1. INTRODUCTION	
1.1. Nanoparticles: characteristics and origins	1
1.1.1. <i>Origin of the nanoparticles: natural vs. man-made</i>	2
1.1.2. <i>Interactions of NPs with living organisms: uptake and transport</i>	2
1.1.3. <i>Interactions of NPs with living organisms: effects at the level of cells and biomolecules</i>	4
1.2. Titanium dioxide: characteristics and applications	4
1.2.1. <i>Human exposure to TiO₂ NPs</i>	5
1.2.2. <i>Toxicity of TiO₂ NPs at the level of organs and organ systems</i>	6
1.2.3. <i>Effects of TiO₂ NPs: interactions with cells and biomolecules</i>	9
1.3. Summary and aims	10
2. MATERIALS AND METHODS	
2.1 Production and characterization of the TiO ₂ nanoparticles	11
2.1.1. <i>Manufacturing</i>	11
2.1.2. <i>Characterizing and suspension preparation</i>	11
2.2. Experimental design: in vivo work	13
2.2.1. <i>Animals and treatment</i>	13
2.2.2. <i>General toxicological investigations: body and organ weights, tissue sampling</i>	15
2.2.3. <i>Cognitive behavioral investigations</i>	15
2.2.4. <i>Electrophysiological investigation</i>	19
2.2.5. <i>Chemical and biochemical measurements</i>	21
2.3. Experimental design: in vitro work	23
2.3.1. <i>Culturing of the cells and exposure to nano-TiO₂</i>	23
2.3.2. <i>Biochemical investigations</i>	23
2.4. Pathomorphological investigations	24
2.4.1. <i>Light microscopic observations</i>	24
2.4.2. <i>Scanning Electron Microscopic (SEM) examinations</i>	24
2.4.3. <i>Transmission Electron Microscopy (TEM) observations</i>	25
2.5. Preliminary experimentation	25
2.6. Data analysis	26
3. RESULTS	
3.1. Summary of the findings of the pilot study	27
3.2. Main experiment – General toxicity in vivo: effects on body and organ weights	27
3.3. Effects of the TiO ₂ nanorods on the rats' lungs and on lung-derived cells	28
3.3.1. <i>Presence of TiO₂ NPs in the lung tissue</i>	28
3.3.2. <i>Biochemical indicators of toxicity of the TiO₂ nanorods present in the lung tissue</i>	31
3.3.3. <i>Presence and toxicity of TiO₂ NPs in lung-derived cells in vitro</i>	33
3.4. Toxicity of the TiO ₂ nanorods on the rats' nervous system	35
3.4.1. <i>Behavioral effects</i>	35
3.4.2. <i>Electrophysiological effects</i>	39
3.4.3. <i>Titanium levels in samples of the brain</i>	41
3.5. Toxic effects of the TiO ₂ nanorods on the kidneys	43
3.5.1. <i>Titanium levels in the kidney samples</i>	43
3.5.2. <i>Histopathological findings in the kidneys</i>	43
4. DISCUSSION	46
5. REFERENCES	52
6. ACKNOWLEDGEMENT	59
7. APPENDIX	60

ABBREVIATIONS

ANOVA	analysis of variance
ASR	acoustic startle response
BBB	blood-brain barrier
CAP	compound action potential
CCL5	chemokine (C-C motif) ligand 5
CINC	cytokine-induced neutrophil chemoattractants
CNTF	ciliary neurotrophic factor
COPD	chronic obstructive pulmonary disease
DLS	dynamic light scattering
ECoG	electrocorticogram
EDS	energy-dispersive X-ray spectroscopy
ELISA	enzyme-linked immunosorbent assay
EP	evoked potential
EPM	elevated plus maze
GFAP	glial fibrillary acidic protein
GM-CSF	granulocyte-macrophage colony-stimulating factor
HE	haematoxylin-eosin
ICP-MS	inductively coupled plasma mass spectrometry
IFN γ	interferon gamma
IL-1, ...	interleukin-1, ...
LIX	lipopolysaccharide induced CXC chemokine
MDA	malondialdehyde
MIP-1 α , -3 α	macrophage inflammatory proteins
NP	nanoparticle
OF	open field
PAA	polyacrylic acid
PBS	phosphate-buffered saline
PM10, PM2.5	aerosol of maximal particle size of 10 or 2,5 μm
PPI	pre-pulse inhibition
ROS	reactive oxygen species
SEM	scanning electron microscopy
sICAM-1	soluble intercellular adhesion molecule-1
SPF	specific pathogen free
TBARS	thiobarbiturate reactive substances
TEM	transmission electron microscopy
TIMP-1	TIMP metalloproteinase inhibitor 1
TNF α	tumor necrosis factor alpha
UV	ultraviolet
VEGF	vascular endothelial growth factor

1. INTRODUCTION

1.1. Nanoparticles: characteristics and origins

The world of nanoparticles (NPs) has gained a great deal of attention in the last ca. 30 years in various fields of research, including life and health sciences. By the generally accepted definition, NPs are particles with not more than 100 nm typical diameter at least in one dimension. Within that, not only approximately cubical or spherical grains but elongated structures such as nano-rods, -wires, -tubes etc. exist, and nano-sized surface patterns on larger objects are also known (Buzea et al., 2007). In the context of environmental load (including workplace environment) NPs are often referred to as ultrafine dust (Oberdörster et al., 2005).

Their size range lends some peculiar characteristics to the NPs, so properties and behavior of the same chemical substance in nano vs. more conventional states can be different – which leads, among others, to biological, and hence, toxicological, interactions not seen with traditional materials, resulting possibly in novel health risks (Kreyling et al., 2006).

This is primarily due to the high surface-to-volume ratio. Crystal structure defects, free valence electrons of surface atoms, adsorbed redox active metal ions or organics, all contribute to high surface reactivity of NPs (Nel et al., 2006). Depending on the NPs' actual surface properties and the substances present in their immediate surroundings, aggregation or agglomeration of the NPs and/or binding of external molecules to the surface will take place – influencing stability of the nanosuspension in liquid or gaseous media, size distribution of the particles, and actual surface reactions (Buzea et al., 2007).

The relationship between elevated level of ambient airborne NPs and human morbidity and mortality has been generally accepted by now (Elsaesser and Howard, 2012). NP content of air samples is seldom measured separately, because the required equipment is costly and no accepted standards exist, but in the level of traditional aerosol load values like PM₁₀ and PM_{2.5}, and even more in the health effects attributable to these (Dockery et al., 1993; Laden et al., 2006), NPs are represented. Aerosol concentration (which necessarily includes NPs) is an important measure of ambient air quality nowadays, with limits set at national (Decree No. 14/2001 in Hungary) and international level (European Council, 2008). The role of NPs in causing various non-communicable diseases like asthma, COPD or ischemic heart disease has been repeatedly analyzed (Donaldson and Tran, 2002). Particulate air pollution has been recognized as an environmental carcinogenic agent (IARC, 2006).

1.1.1. Origin of the nanoparticles: natural vs. man-made

Natural phenomena generating NPs are, among others, forest and bush fires, volcanoes, sea spray, as well as erosion of rocks and soil. There is also a natural emission of gaseous substances that can react to produce NPs in the atmosphere (e.g., volatile terpenoids of coniferous trees).

Among man-made NPs, by-products of various technological procedures, acting as pollutants, and purposefully produced nanomaterials are to be distinguished.

The main sources of man-made pollutant NPs are combustion, other high temperature processes (metal casting, welding, etc.: Antonini, 2003) and working on solid materials.

Intentional manufacturing of NPs, for scientific studies or practical application in various fields including consumers' goods – that is, nanotechnology – has been gaining much importance in the last two decades. In the meta-analysis by Debia et al. (2016) occupational exposure to nanomaterials like carbon nanotubes and nanofibres, metal oxide NPs (of Al, Ti, Si, Fe, Zn) and nano-clay was described as likely.

Engineered nanomaterials are also becoming part of everyday life, because several NP-containing products from cosmetics and suntan lotions to tennis balls, paints and stain-resistant clothing, are commercially available (Kahru and Dubourguier, 2010). This very broad spectrum of application, and concomitant human exposure, raise the question of health risk. Here, a major problem is the lack of toxicity data for most manufactured NPs (SCENIHR, 2009) – and this is why nanotoxicology, an interdisciplinary field related to both environmental hygiene and nanotechnology, emerged (Suh et al., 2009). The US Environmental Protection Agency (2003) announced an urgent need for research data on toxicology of manufactured nanomaterials and human exposure and bioavailability. The European Agency for Safety and Health at Work (2009) listed workplace exposure to NPs among the major emerging risks related to occupational safety and health.

1.1.2. Interactions of NPs with living organisms: uptake and transport

Any toxic effect is the final outcome of interaction of an external agent and the exposed living organism. In case of humans and NPs, the first question is how the particles enter the body.

The most likely entrance is, first of all for environmental pollutant NPs but partly also for those from nanotechnological applications, by inhalation of air containing a nano-aerosol. NPs are either deposited in the nasopharynx or get down to the alveoli (ICRP, 1994), and settle mainly due to free diffusion driven by collision of the particles with air molecules (Oberdörster et al., 2005). The deposited NPs, in contrast to microscopic and even larger particles, are not held back by biological barriers like the alveolar and capillary wall, and reach other target organs

partly by being phagocytosed and transferred along the lymphatic system, but partly by different mechanisms including transcytosis (Oberdörster et al., 2005). NPs can cross respiratory epithelium and reach the interstitium by means of caveolae (50-100 nm sized invaginations of the cell membrane, serving endo- and transcytosis of a number of molecules and microstructures: Razani and Lisanti, 2001) formed around NPs. Having crossed the alveolar and capillary membrane, NPs are distributed throughout the body by the circulation (Oberdörster et al., 2005). The NPs' passage across the capillary wall is promoted by endothelial leakiness. If an NP is small enough to fit in the adherens junction (desmosome) between two endothelial cells, the bond between the VE-cadherin molecules (vascular endothelial cadherin, transmembrane glycoprotein molecules linking the cells) will be disrupted, and the cells will retract leaving a broader gap between, promoting the passage of larger particles also (Boland et al., 2014). Choi et al. (2010) studied the effect of NP diameter and surface charge on migration and distribution of the particles after pulmonary instillation in rats. Only NPs below 34 nm size showed rapid transepithelial movement to the interstitium and further to local lymph nodes and finally to the bloodstream, provided their surface had no net positive charge. The fate of very small (<6 nm) particles was similar but these were also rapidly excreted by the kidneys.

Gastrointestinal and dermal absorption of NPs may seem less important than inhalation, but deserves attention because of presence of engineered NPs in foods and skin care products (Groh et al., 2017; Wiesenthal et al., 2011) and of environmental background level of NPs possibly reaching drinking water (Abbott Chalew et al., 2013; Giovanni et al., 2015). Depending on size and surface charge, NPs can enter the intestinal epithelium and further the blood but are possibly removed in the liver. Peyer's patches and local lymph nodes are supposed to be involved in the elimination. In certain chronic gastrointestinal ailments, e.g. Crohn's disease, the role of ingested NPs has been supposed (Buzea et al., 2007). Dermal uptake of NPs is unlikely through an intact keratinous layer but has been demonstrated in cases when the human or animal skin was broken or repeatedly flexed (Oberdörster et al., 2005). The local lymphatic system is involved in the transport of NPs also here. Nohynek and Dufour (2012) concluded from a literature survey that personal care products containing NPs pose, when applied on the skin, no health risk attributable to the presence of NPs. Wiesenthal et al. (2011) meant, however, that knowledge on this issue was far from being complete. And, after NPs penetrate the outermost layers, all peripheral nerve endings can serve as starting points for transport of NPs along their axons to more central parts of the body and finally to the central nervous system (Oberdörster et al., 2005).

1.1.3. Interactions of NPs with living organisms: effects at the level of cells and biomolecules

NPs have large specific surface area which is also very reactive (due to reasons described above, see Nel et al., 2006). In the aqueous microenvironment of living tissues this leads to generation of reactive oxygen species (ROS). The resulting oxidative stress, one of the most typical effects of NPs, can induce damage to biomolecules in case the cells' antioxidant defence mechanisms cannot cope with.

In proteins, certain amino acid side chains undergo oxidation by ROS. The resulting carbonylated proteins may have a role in various chronic diseases including those of the central nervous system like Alzheimers's disease (Dalle-Donne et al., 2003). Lipids, especially if unsaturated, are sensitive to oxidation. Attacked by oxidative radicals, unsaturated fatty acids break down to peroxidated lipid radicals (attacking further molecules) and to end products like malondialdehyde (MDA) and 4-hydroxy-nonenal (Valko et al., 2005). These reactive molecules can, e.g., form DNA adducts leading to genotoxicity; and are measurable biomarkers of oxidative damage (Serbinova et al., 1992).

Using a murine macrophage cell line (RAW 264.7) and Diesel exhaust extract, Xiao et al. (2003) described a multi-level mechanism of cellular defence against oxidative stress. The first level means induction of antioxidative and metabolic enzymes (glutathione synthetase, glutathione-S-transferase, hemoxygenase, etc.) belonging to normal antioxidant defence. Are these insufficient, the next level comes into play with activation of the mitogen-activated protein (MAP) kinase and nucleic factor-kappaB (NF- κ B) pathways, ending up in release of inflammatory cytokines. The highest level of oxidative stress then leads to mitochondrial damage and cytotoxicity, where the direct effect of NPs on mitochondria also has a role. From a mechanistic perspective, ROS generation and oxidative stress is the best developed paradigm to explain the toxic effects of nanoparticles. Donaldson and Tran (2002) described direct relationship between the surface area, ROS generating capability, and proinflammatory effects of nanoparticles.

The biochemical consequences of ROS generation, such as lipid peroxidation, or changes in antioxidant enzyme activity and in expression of cytokines, are potential biomarkers of NP toxicity (suitable even for toxicity screening of airborne particles: Ayres et al., 2008).

1.2. Titanium dioxide: characteristics and applications

Titanium dioxide (TiO₂) is the derivative with the highest practical importance and broadest field of application of the transition metal titanium (Ti). It is a white, odorless, non-water

soluble solid of high chemical stability and high melting temperature. It exists in several crystal forms, the two major ones being rutile and anatase (Shi et al., 2013).

TiO₂ has been used first of all as white pigment. This consists mostly of 0.2-0.4 μm grains, but contains a nano-sized fraction, too (Warheit and Donner, 2015); and is in use also in the food and pharmaceutical industry (food additive code: E171).

Nanoparticulate TiO₂ has, in various shapes (grains, rods, wires, tubes) a broad range of application. One with direct human contact is in skin-protective products against solar UV radiation. TiO₂ NPs in such “physical sunscreens” reflect UV-B, and to a lesser extent UV-A, rays. Radiation absorbed by TiO₂ NPs (first of all of anatase form) results in excitation and generation of free radicals. This is undesired on the skin but is utilized in applications like self-cleaning windows and building facades (Chen and Poon, 2009), self-disinfecting fabrics and surfaces (Dastjerdi and Montazer, 2010), etc.

1.2.1. Human exposure to TiO₂ NPs

Human exposure to TiO₂ NPs may occur during manufacturing, processing, and use; in form of aerosols, suspensions or emulsions. The major routes with health relevance in workplaces are inhalation and dermal exposure, both taking place mostly while handling the nano-TiO₂ semi-products (Shi et al., 2013). Worldwide production of several million tons of TiO₂ (including both microscopic and submicroscopic particles) suggests occupational risk. The National Institute of Occupational Safety and Health published a limit of 0.3 mg/m³ for ultrafine (nanoparticulate) TiO₂ in the workplace atmosphere (CDC-NIOSH, 2011). Actual measurements proved temporary exceedance of this limit during production and packaging of nano-TiO₂ (Koivisto et al., 2012) while model calculations showed real health risk (Ling et al., 2011). In an earlier period, workplace exposure to airborne TiO₂ resulted in decreased ventilatory capacity and pleural thickening (Garabant et al., 1987), and neurological symptoms were also observed (Oleru, 1987).

Non-occupational exposure by TiO₂ NPs is most likely dermal or oral. Processed foods (typically sweets and chewing gums), toothpastes, etc. contain TiO₂ as colorant (Weir et al., 2012). An evaluation by the European Food Safety Authority stated that the daily uptake of TiO₂ pigment can reach 30 mg/kg body weight in children (consuming much sweets containing artificial colorants); and of that, at ca. 3% – 1 mg/kg body weight – may be nano-sized (EFSA, 2016). Presence of nano-TiO₂ in drinking water, resulting from previous environmental release (e.g. from sunscreens: Gondikas et al., 2014) is possible, but most likely not harmful (Giovanni et al., 2015).

Dermal exposure of humans may be of interest due to presence of TiO₂ NPs in sunscreen products as mentioned above. In the review by Shi et al. (2013) penetration of TiO₂ NPs (and other inorganic NPs) through intact human skin is declared unlikely. In certain studies, however, TiO₂ NPs reached the viable epidermis and dermis of humans after 2-6 weeks of daily application (Tan et al., 1996) but had no harmful effect. In contrast, nano-TiO₂ penetrated hairless skin of mice in 4 weeks and reached the liver (Wu et al., 2009).

1.2.2. Toxicity of TiO₂ NPs at the level of organs and organ systems

1.2.2.1. Effects of TiO₂ NPs in the airways and lungs

Inhalation is a major route of exposure to any NP, including nano-TiO₂ (Shi et al., 2013), and corresponding occupational health damages (such as decreased ventilatory capacity: Garabant et al., 1987) have in fact been reported. There are a few reports on occupational nano-TiO₂ inhalation where alterations or manifest health damage could be ascribed to the exposure. Zhao et al. (2018) investigated factory workers exposed to airborne TiO₂ dust with high NP content. Compared to non-exposed employees of the same factory, the exposed showed significant alterations in certain serum biomarkers of oxidative stress, inflammation, and lung damage. Similarly, Pelclova et al. (2016) found elevated oxidative stress markers in the exhaled breath condensate of nano-TiO₂ exposed workers. *In vitro* analogs of the mentioned studies, performed on human-origin cell cultures, verified the ability of TiO₂ NPs to induce oxidative damage and inflammatory response (Ursini et al., 2014). These reports are in certain contradiction with earlier epidemiological studies which revealed no significant excess morbidity or mortality due to inhalation of TiO₂ NPs at workplaces (CDC-NIOSH, 2011) and no increased risk of lung cancer (Boffetta et al., 2001; Ramanakumar et al., 2008).

In rat lungs, Yoshiura et al. (2015) evoked transient inflammation with activation of cytokines and antioxidant enzymes by a single intratracheal application of TiO₂ NPs. Using true inhalation exposure with nano-TiO₂ in rats, NP-laden alveolar macrophages (Kwon et al., 2012) and increased levels of various cytokines and cytotoxicity markers (Noël et al., 2013) were observed already after a single dose; while 6 hours of inhalation on 5 consecutive days induced neutrophilic inflammation (Ravenzwaay et al., 2009). Pujalté et al. (2017) reported that following a single session of TiO₂ NP inhalation (anatase, ca. 25 nm) in rats, most of the material remained in the lungs. Levels in blood and in other organs inclusive brain were 10 to 100 times lower than in the lungs. Oxidative stress was transiently present. Also with a single instillation, Kobayashi et al. (2009) found particle size dependent inflammation (stronger for smaller particles) and tissue damage in the rats' lungs after 24 hours that decreased in a week.

The findings of Sager et al. (2008) were similar – more cytotoxicity and inflammation by nano- than by micro-sized TiO₂ particles – underlining that surface area is (as stated earlier by Oberdörster, 2000) decisive in the extent of biological effects of NPs. These authors also reported more translocation of nano-TiO₂ from the alveolar space to the interstitium and macrophages.

1.2.2.2. Effects of TiO₂ NPs on the nervous system

The possible effects of NPs on the nervous system are of especial interest for two reasons, one being the role of an intact nervous system in the healthy life of animals, and even more of humans; and the other, the sensitivity of the nervous system to the biological effects of NPs. A healthy blood-brain barrier (BBB) is able to prevent foreign particles from entering the brain. All the same, NPs of various compositions – including TiO₂ – were detected in the brain of rats after application through the airways (Kreyling et al., 2006). Some published experiments with TiO₂ NPs verified access to the brain after application to the airways, together with damage to the blood-brain barrier (in rats: Liu et al., 2013); while others found that most of the nano-TiO₂ applied to the airways remained in the lungs (also in rats: Baisch et al., 2014). In the review by Song et al. (2015) the listed possible ways of NP to the brain are: across the BBB, along the olfactory and other nerves, and across the placenta during fetal development; but the size and other properties (hydrophilic or hydrophobic surface etc.) strongly influence whether the NPs in fact reach the brain.

According to the review by Czajka et al. (2015), rat-based models of nervous system effects of TiO₂ NPs are, as opposed to e.g. mouse models, scarce in the literature. Inhalation exposure of rats to 10 mg/m³ nano-TiO₂ aerosol (daily 6 hours, 5 days a week for 4 weeks) resulted in increased level of inflammation markers and decreased expression of synaptophysin in the brain without relevant deposition of Ti (Disdier et al., 2017). In young rats exposed during lactation via the milk of dams who were treated orally, impaired synaptic plasticity in the dentate gyrus and significant Ti deposition in the hippocampus were found (Gao et al., 2011). When adult rats received oral administration of TiO₂ NPs, decreased brain acetylcholinesterase activity, together with increased GFAP reactivity and interleukin-6 level, was observed (Grissa et al., 2016). However, as written above, others found that nano-TiO₂ applied in the airways failed to reach the brain of rats (Baisch et al., 2014).

Functional alterations, possibly resulting from access of TiO₂ NPs to the brain, have been described at the level of electrophysiological changes only a few times up to now. Using murine frontal cortex neuronal networks cultured *in vitro*, uptake of nano-TiO₂ by the cells and massive

depression of spike activity was found (Gramowsky et al., 2010). Also in mice, 90 days of oral nano-TiO₂ treatment caused neuronal degeneration, dose-dependently reduced hippocampal long-term potentiation, and impaired spatial memory and locomotion (Ze et al., 2014). Similar exposure for 60 days impaired spatial recognition and altered neurotransmitter levels in mice (Hu et al., 2010). In young Wistar rats, TiO₂ NPs given by intraperitoneal injection for 20 days resulted in increased anxiety, indicated by spending less time in the open arms of an elevated plus maze. There was elevated Ti level in brain and other organs, and elevated blood enzyme levels indicating cellular damage (Ben-Younes et al., 2015; Amara et al., 2013).

Regarding humans, workers exposed to airborne titanium-based pigment particles at the workplace showed some neurological symptoms (Oleru, 1987). The majority of results suggesting human nervous system affection was achieved, however, in *in vivo* investigations on cultured cells of human origin. Coccini et al. (2015) treated human-derived neuronal (SH-SY5Y) and glial (D384) cells with TiO₂ NPs, and found decreased mitochondrial function and cell membrane integrity. Also in SH-SY5Y cells, Valdiglesias et al. (2013) found no decreased viability but could verify cellular uptake of the NPs and apoptosis.

1.2.2.3. Effects of TiO₂ NPs in other organs

For the exposed organism, NPs are xenobiotics. Hence, their effects on organs involved in metabolism and excretion, that is, liver and kidneys, are of interest.

In mice treated by a single intragastric administration, nano-TiO₂ (of <10 nm diameter) was found to be deposited in the kidneys, causing increase of organ weight, inflammation, cell death and dysfunction. NF- κ B was activated by TiO₂ NP exposure, enhancing the expression of tumor necrosis factor alpha (TNF- α), and various inflammatory interleukins (Gui et al., 2013). Similar effects were seen by Fadda et al. (2018) in rats on 3 weeks of oral exposure by TiO₂ NPs (size not specified): increased level of TNF- α , IL-6 and C-reactive protein, together with decreased renal function, and histological damage to glomeruli and tubules. In the latter paper, the authors ascribed these damages to oxidative stress as they were significantly reduced by antioxidants applied together with nano-TiO₂. On a single iv. application of nano-TiO₂ to rats, oxidative stress was observed in liver and kidney, with more severe damage in the latter (González-Esquivel et al., 2015). Also in rats, on application of 20-30 nm TiO₂ NPs subcutely ip., Ben-Younes et al. (2015) observed accumulation of Ti in the liver and kidneys (beside brain) but noteworthy damage only in the liver.

1.2.3. Effects of TiO₂ NPs: interactions with cells and biomolecules

These organ-level effects of TiO₂ NPs result from interactions at the cellular and molecular level. Of these, the most basic and general is induction of oxidative stress (Grande and Tucci, 2016), a manifestation of the NPs' surface reactivity (Nel et al., 2006). When excited, electrons move from the valence band to the conduction band of the TiO₂ crystal structure, and both surplus electrons and the "holes" left by them contribute to the formation of ROS (Li et al., 2014). Crystal forms of nano-TiO₂ that are more efficient in *in vivo* ROS generation (e.g., anatase) are also more cytotoxic, even in absence of UV light excitation (Sayes et al., 2006). ROS generated by TiO₂ NPs include superoxide anion, hydroxyl radical and hydrogen peroxide.

The first step in NP-cell interactions is usually some form of internalization. TiO₂ NPs were shown to enter cells by clathrin-mediated endocytosis, caveola formation, and macropinocytosis, depending on cell type (glia cells: Huerta-Garcia et al., 2015; prostate cancer cells: Thurn et al., 2011; dorsal root ganglion cells: Erriquez et al., 2015). Following uptake, TiO₂ NPs are mostly found in lysosomes, but these are likely damaged, due to the tendency of TiO₂ NPs to form aggregates sufficiently big to damage lysosomes mechanically, as well as due to lipid peroxidation induced by the NPs and subsequent membrane damage. Lysosomal membrane permeabilization then releases enzymes, such as cathepsin B, activating caspases (constituents of inflammasomes) that further convert interleukin-1beta to its active form, ending up in apoptosis (Boland et al., 2014). The released enzymes also attack the outer mitochondrial membrane, and mitochondrial damage contributes to oxidative stress (Stern et al., 2012).

1.3. Summary and aims

Literature data cited above clearly show that exposure of humans to TiO₂ NPs can take place both in occupational settings, and in the residential environment, or during free-time activities. It is also clear that certain properties of the TiO₂ NPs suggest harmful effects on various organs and organ systems of humans or animals – due to involvement in uptake and elimination (lungs, kidneys, liver) or to especial sensitivity (nervous system) – but the available reports on such effects are not yet conclusive.

At the Department of Public Health, the toxicity, first of all neurotoxicity, of metal oxide NPs has been investigated for over 10 years. Based on the experience gained, and on the properties and possible effects of TiO₂ NPs outlined above, it was decided to investigate in the present PhD the alterations evoked by TiO₂ NPs work with a complex approach. By treating rats subacutely via the airways, and applying morphological, chemical, biochemical as well as behavioral and electrophysiological methods, answer to the following questions was sought:

- Is it possible to create effective internal TiO₂ NP load in the treated rats by intratracheal instillation?
- Do the TiO₂ NPs cross biological barriers, reach the circulation and/or distant organs (including essential targets such as brain, liver, kidneys), and show deposition in the latter?
- What alterations – morphological and/or biochemical-molecular – are elicited in the gate organ, the lungs?
- Is the set of behavioral and electrophysiological methods, applied previously to study the effects of other metal oxide NPs, suitable to examine the neurotoxic effects of TiO₂ NPs?
- What are the main functional alterations detectable at the level of cognitive behavioral and electrophysiological phenomena?
- How are the kidneys, as possible organs of excretion, affected by the internal TiO₂ NP load?
- What is the relationship between the observed morphological (cellular or subcellular), as well as biochemical and neuro-functional, alterations and Ti or TiO₂ NP load detected in the corresponding organs?
- What implications have the results, presented in this thesis, to human, primarily occupational, health risk?

2. MATERIALS AND METHODS

2.1 Production and characterization of the TiO₂ nanoparticles

The TiO₂ NPs were manufactured and examined at the Department of Applied and Environmental Chemistry, University of Szeged Faculty of Science and Informatics, using chemicals obtained from Sigma-Aldrich Hungary (Budapest, Hungary). Based on preliminary experimentation (see 2.5.) it was decided to work with rod-shaped TiO₂ NPs.

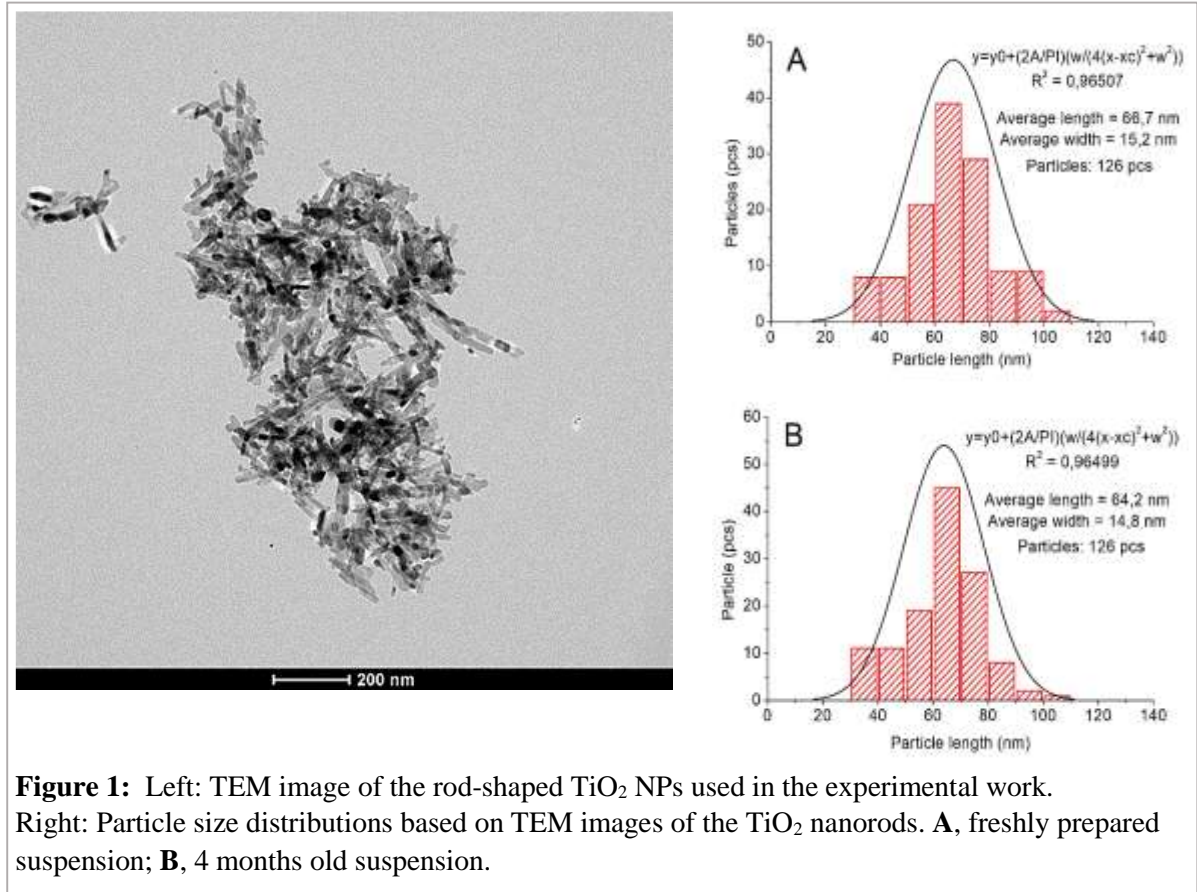
2.1.1. *Manufacturing*

Nanorods of TiO₂, with size of ca. 15x65 nm, were synthesized from titanate nanotubes as intermediate products in a simple alkali hydrothermal method as follows: 1 L of 10 M NaOH solution and 50 g of TiO₂ nano-powder (Degussa P25) were mixed in a stainless steel teflon-lined autoclave for 24 h at 428 K using a continuous rotation at 3 rpm. The as-prepared TiO₂ nanostructures were washed thoroughly with deionized water to neutral pH, then with 0.1 M HCl several times, and finally with water again to obtain a neutral, salt-free product. Finally, the TiO₂ nanotubes obtained were heated at 600°C for 1 hour in normal air, whereupon the desired nanorods evolved.

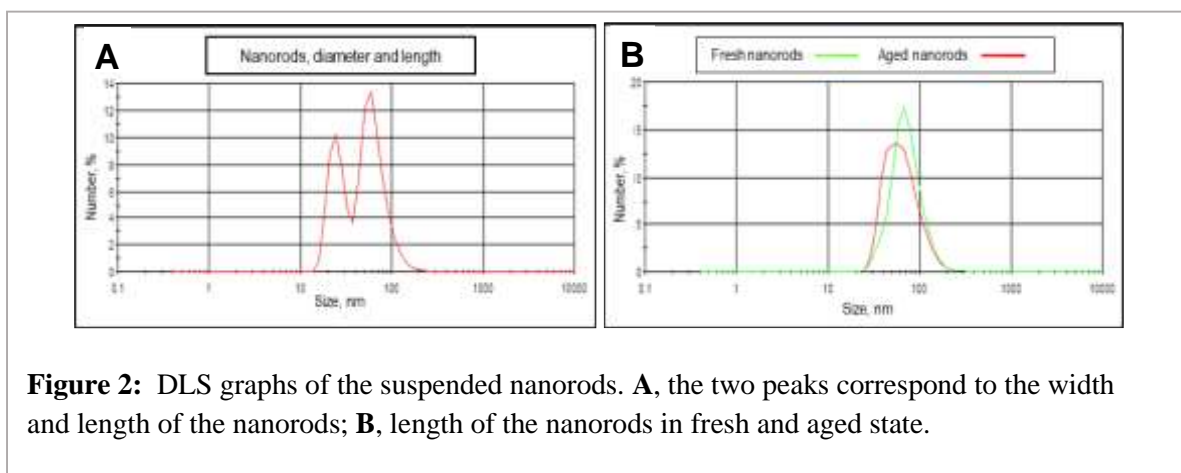
2.1.2. *Characterizing and suspension preparation*

The TiO₂ NPs were characterized primarily by size determination using transmission electron microscopy and dynamic light scattering. The TEM image shown in Fig. 1, left, confirmed that the prepared nanomaterial consisted of particles in the desired shape and size range, and that they were largely uniform.

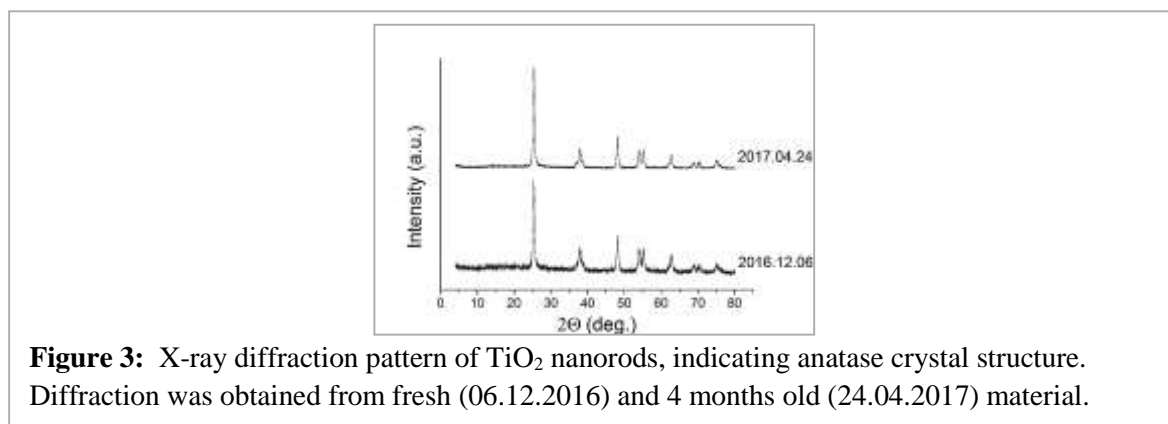
Size was quantified by measuring length and width of the nanorods on the TEM images. The size distribution plots, based on the Lorentz (Cauchy) distribution, proved that the size of the synthesized TiO₂ NPs was largely uniform with a narrow distribution range (Fig. 1, right).



Dynamic light scattering (DLS; Berne and Pecora, 2000) was used to examine the actual size of particles in the nanosuspension to be used for treating the rats and cultured cells (Fig. 2). The results were congruent with those obtained by TEM.



Crystal structure, another feature of importance in the biological effect of TiO₂ NPs, was determined by X-ray diffraction. A mostly anatase-type structure was verified (Fig. 3) based on information by the International Centre for Diffraction Data (ICDD, 2018).



The nanomaterial was suspended in phosphate-buffered saline (PBS) containing 1% polyacrylic acid (PAA, MW ~ 5000) with pH set to 6.8 (this was not strictly physiological but pH had to be optimized with regard to both suspension stability and tolerability by the rats). PAA is often used in biomedical applications (for previous experiences of our laboratory, see Oszlanci et al., 2010, 2015), and is even a potential candidate as vaccine component (Topuzogullari et al., 2013). In preparing the suspension, a 200 W ultrasonic device (Hielscher UP200HT; Hielscher, Teltow, Germany) was used, and the suspension was treated by the same device before daily application to the rats.

2.2. Experimental design: *in vivo* work

The experiments performed included both *in vivo* work with rats and *in vitro* work using cultured cells.

2.2.1. Animals and treatment

Young adult male SPF Wistar rats (CrI:WIBr; 6 weeks old, 170±20 g body weight) were used, obtained from Toxi-Coop Ltd. (Budapest, Hungary). The rats were kept, two in a cage, in an animal house conform with the requirements of good laboratory practice (GLP: 12-12 hours light/dark cycle with light on at 06:00; temperature 22±3 °C, 30- 70% relative humidity); and could consume unlimited amount of standard rodent food (Ssniff R/M-Z+H, also from Toxi-Coop Ltd.) and water. After one week of acclimation, the rats were randomized to treatment

groups according to the scheme given in Table 1. Randomization was based on body weight and pre-treatment open field performance (see below, 2.2.3.3).

During the whole *in vivo* study, the principles of the Ethical Committee for the Protection of Animals in Research of the University of Szeged were strictly followed. The methods used were licensed by Csongrád County Government Office, Directorate for Food Chain Safety and Animal Health under No. XXI./151/2013.

Table 1: Scheme of the *in vivo* experiment

Duration and treatment scheme:	5 days per week, altogether 28 treatment days, resulting in 6 weeks	
Rat groups and treatments:	Untreated control; <i>C</i> Vehicle control; <i>VC</i> Treated, low dose; <i>LD</i> Treated, medium dose; <i>MD</i> Treated, high dose; <i>HD</i>	Saline, 1 mL/kg b.w. PBS + 1% PAA, 1mL/kg b.w. TiO ₂ nanorods, 5 mg/kg b.w. TiO ₂ nanorods, 10 mg/kg b.w. TiO ₂ nanorods, 18 mg/kg b.w.
Investigations:	General toxicology: Cognitive behavior: Electrophysiology: Chemistry, biochemistry: Pathomorphology:	Body weight gain Organ weights Climb test Elevated plus-maze Open field Acoustic startle response and pre-pulse inhibition Electrocorticogram Cortical evoked potentials Nerve compound action potential Tissue Ti levels Oxidative stress: thiobarbiturate reaction, catalase activity Detection of cytokines: Array kit Visualizing NPs and NP-laden macrophages: Light microscopy and TEM Verifying Ti in tissue slices: EDS

Abbreviations: PBS, Phosphate-buffered saline; PAA, polyacrylic acid; TEM, Transmission electron microscopy; EDS, Energy dispersive spectroscopy.

The rats were exposed to TiO₂ by intratracheal (it.) instillation. Administration was performed, according to the scheme in Table 1, always between 8:00 and 10:00 am; and required brief anesthesia using diethyl ether (applied in a glass jar with air-tight lid). The completely anesthetized rat was suspended on a board tilted at 60°. The trachea was illuminated transdermally, tongue pulled forward with a pair of non-traumatic forceps, and a custom-made laryngoscope was used to gain access to the glottis. TiO₂ nanosuspension was instilled into the

trachea by means of a 1 mL syringe and 1.2 mm diameter plastic tubing inserted between the vocal chords. The volume applied was 1 mL/kg b.w. Before taking up the suspension, an equal quantity of air was drawn into the syringe and was pushed out after the suspension to assure that the whole amount was delivered into the trachea. This technique was identical to that in Oszlanczi et al. (2010, 2015). The doses were determined based on the outcomes of preliminary experiments (see 2.5. as well as papers No. III and IV in Appendix).

2.2.2. General toxicological investigations: body and organ weights, tissue sampling

The rats' body weight was measured every morning, before treatment, to determine the exact doses to be instilled (see above), and to observe the effect on body weight gain. Body weight gain for one-week periods and for the whole experiment were calculated. Any sign of toxicity (e.g. rough fur, hunched back, unusual aggressive behavior, etc.) was observed and noted.

After all behavioral and electrophysiological recordings (see below) had been done, the rats were sacrificed by an overdose of urethane (twice the anesthetic dose, see 2.2.4.1.), and were dissected. After opening the abdominal and thoracic cavity, 2-3 mL blood was taken from the left heart ventricle for measuring Ti level and certain oxidative stress parameters. The rats were then perfused with 300 mL saline of 4°C temperature to wash blood from the organs. During autopsy, the most important organs including brain, cerebellum, hippocampus (on both sides), heart, liver, lungs, spleen, kidneys, adrenals, and thymus were weighed, and relative organ weights (to 1/100 body weight) were calculated. Brain and liver samples were shock-frozen in liquid nitrogen and stored at -20°C for subsequent biochemical and chemical measurements; while one of the kidneys and adrenals, and one half of the lungs were preserved frozen as above, and the other parts were preserved in 4% neutral buffered formalin for histopathological examinations by means of light and electron microscopy.

2.2.3. Cognitive behavioral investigations

2.2.3.1. Climb test

Climb (or grip strength) test was used to assess the rats' motor function (Feng et al., 2014). A wooden rod of ca. 8 mm diameter and rough surface was fixed horizontally in 60 cm height above a tray lined with a layer of wood chips litter. The rats were, one by one, made grasp the wooden rod with their front paws and let hang free. Four trials were made with each rat in line, and the length of time until falling was measured and averaged. This test was done before starting of the treatment period, and on the last day of the treatment period, ca. 2 hours after

instillation. For each rat, the average time-to-fall on the 4th week was divided by the corresponding data of the 0th week, and this ratio was used to quantify the effect of nano-TiO₂.

2.2.3.2. Elevated- plus maze test (EPM)

This test is applied for understanding the biological basis of emotionality related to learning and memory, pain, hormones, addiction and withdrawal, etc. (Bannerman et al., 2004). The unconditioned responses in the EPM task are attributed to the spontaneous fear elicited by the setting. Rodents tend to avoid open spaces so they show clear preference for the closed vs. the open arms (Walf and Frye, 2007). However, some learned behavior may develop during the test, leading to gradual increase in the avoidance behavior – so EPM might not purely be a test of unconditioned responses (Carobrez and Bertoglio, 2005). In our work, EPM test was performed on the same day with the open field test, with ca. 30 min interval between the two. Our EPM, elevated to 50 cm height above the floor, consisted of two open arms (50x10 cm) and two enclosed arms (50x10 cm, with 40 cm high side walls and open roof); the two open arms were opposite to each other. The rats were individually placed at the junction of the four arms (10x10 cm central area), facing the open arm farther from the examiner. During the 10-min test period, the animals could move freely in all arms. The sessions were recorded on digital video and evaluated afterwards. Aspects of evaluation were the number of entries into the closed and open arms, to the end of the open arms, and to the central area of the maze; an entry was defined as the step of all four feet into one arm or the central area. Length of time spent in the areas specified above was measured also, as well as the time elapsing until entering the first open arm, the length of first stay in an open arm and at the end of the open arm.

2.2.3.3. Open field test

The rats' spontaneous motility was tested in an open field (OF) apparatus (Conducta 1.3 System; Experimetria Ltd., Budapest). OF test is a standard method to assess spontaneous exploratory motor activity in experimental animals and its changes upon action of exogenous chemicals (Pryor et al. 1983) also included in the guideline for neurotoxicity testing issued by the Organisation for Economic Co-operation and Development (OECD, 2004).

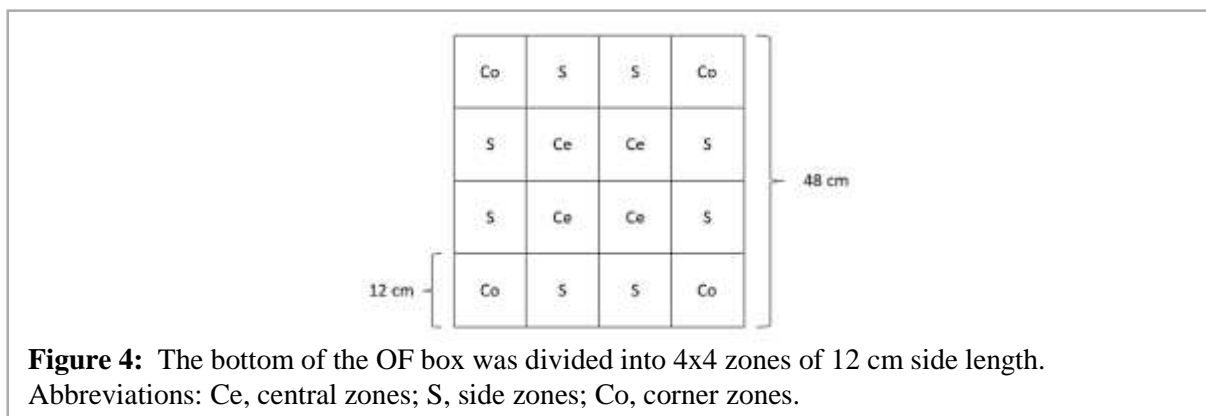
This test provides a variety of behavioral information ranging from general ambulatory motility (spontaneous exploration, stereotypical movements) to emotionality (e.g. degree of anxiety, level of fear). Ambulation near the wall vs. in the center, defecation frequency, and spontaneous activity in the 1st minute, are useful indicators of the level of anxiety.

Exploratory activity depends on mesolimbic and mesocortical dopaminergic transmission (Fink and Smith, 1980), and on the activity of motor control centers including globus pallidus, substantia nigra, and the cerebellar nuclei. Motivation and emotionality, influencing the outcome of both OF test and acoustic startle response test (see below, 2.2.3.4.) is under control by dopamine containing neurons of the ventral tegmental area (Gifkins et al., 2002).

Locomotor activity may be influenced by chemical agents acting on neuronal receptors or causing neuron damage. Further influencing factors include time of day, level of arousal, environmental novelty, age, and stress level; it is hence crucial to carefully select and ensure permanent test conditions and circumstances.

The test was performed before starting the treatment (results used for randomization, as mentioned above), in the middle of the treatment period (3rd week) and when it was over (6th week; typically on the day following the last treatment); always between 8 and 14 o'clock. The animals were first accommodated to the testing room for 20–30 min, and then were placed one by one into the center of the OF box (equipped with two arrays of infrared light gates at floor level and in 12 cm height; for floor size see Fig. 4). During the 10-min session, the system recorded the interruptions of the infrared beams, and these data were computed to event counts and summed time of the basic activity forms – horizontal, local, vertical activity and immobility – as well as run length of ambulation. More than 40 mm shift in the location of interrupted beams at the floor level during a time unit of 1 s was interpreted as horizontal activity (ambulation); less shift, as local activity; and no shift at all, as immobility. Rearing was recorded if beams at floor level and at the higher level were interrupted simultaneously.

These parameters were calculated for the whole session or for the 1st minute, as well as for the whole area or for separate zones shown in Fig. 4. The 1st minute was of interest because exploratory activity diminishes over time; and the rat's time of presence in the corner and side zones vs. the center is an indicator of level of anxiety (Griebel and Holmes, 2013). By exposing the rats to the same OF in the 3rd and 6th week, memory for the novel experience could be tested.



During the 6th week exposure, lower spontaneous exploratory activity indicated better memory for the OF. After each rat, the OF box was wiped with a neutral detergent.

2.2.3.4. Acoustic startle response and pre-pulse inhibition

Acoustic startle response (ASR) is a fast involuntary contraction of the major muscles of the body, generally leading to extension of the fore and hind paws followed by muscle flexion into a hunched position, evoked by unexpected and intense acoustic stimuli (Koch and Schnitzler, 1997). Changes of ASR on systemic application of test substances are widely used to assess the substances' effects on sensorimotor reactivity in animals including rats, but also in humans (Koch, 1999).

The sensory neural reflex pathway of ASR starts with the auditory nerve and continues to the cochlear nucleus, which projects to a small cluster of giant neurons in the ventrocaudal part of the nucleus reticularis pontis caudalis (nRPC) of the reticular formation via the lateral lemniscus (and paralemniscal zone of the ventral lateral lemniscus). Motor outputs are generated in the reticular pontine nucleus (RPC) projecting to the ventral tegmental area. RPC giant neurons activate hundreds of motoneurons in the brain stem and along the length of spinal cord. This basic reflex is modulated by higher brain centers (e.g. amygdala and forebrain: Yeomans and Frankland, 1995). Presenting a lower intensity acoustic stimulus prior to the ASR eliciting stimulus attenuates the response to the latter. This phenomenon, called pre-pulse inhibition (PPI), is influenced by forebrain centers, and provides a measure of sensorimotor gating. PPI is modulated by cognitive and emotional contexts such as fear and attention (Ramirez-Moreno and Sejnowski, 2012).

The test was performed within a sound-proof plexiglas chamber (16×28×18 cm; Responder X System, Columbus Instrument, Ohio, USA), into which the rats were placed, one by one, on the top of a metal load cell platform. A continuous white background noise (65 dB) was delivered from a loudspeaker mounted 10 cm from the test cage. Following 10-15 min adaptation, the rats were exposed to a series of 10 equal intensity sound bursts (startling stimuli in ASR-alone trial; 5 kHz, 110 dB, 200 ms, 15 s inter-trial interval). The vertical force associated with the startle response was measured by the load cell (time course of the force is shown in Fig. 6). One ASR session of 10 trials was performed.

Following a 15-minute recovery, another session of 10 stimuli was started with 15 s intervals. This time, a lower-amplitude stimulus, a pre-pulse (1 kHz, 73 dB, 500 ms; see above) was presented just before the startling stimulus (inter-stimulus time: 200 ms) to elicit PPI.

In both tests, a muscle twitch of the rat, exerting more than 50 g force on the platform was accepted as “noise-positive” response. Such events were counted, and three parameters of them were calculated from the recorded force-time curve: latency, peak amplitude, and time to peak amplitude (see Fig. 5). The effect (%) of acoustic startle on the sensorimotor gating was calculated as the ratio of the averaged parameters (defined above) obtained with and without pre-pulse [(PPI/ASR)x100].

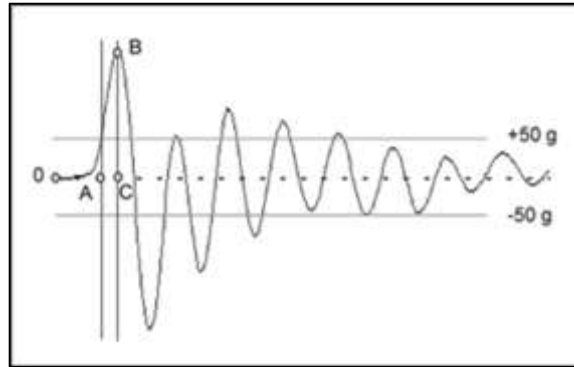


Figure 5: Measurements on the force-time curve of an ASR record. Latency time, 0 – A; peak amplitude, B –C; time-to-peak, 0 – C.

2.2.4. Electrophysiological investigation

2.2.4.1. Anesthesia and preparation

Preparation and electrophysiological measurement was done in terminal anesthesia using urethane (1000 mg/kg b.w. ip.: Koblin, 2002). The level of anesthesia was checked by the hind leg withdrawal reflex (similarly to that in Zandieh et al., 2003); if there was no reaction, the rat was ready for preparation.

The head of the rats was fixed in a holder frame, skin opened by a mid-sagittal cut, soft tissues removed, and the left hemisphere was exposed by removing the temporal bone along the inner circumference by means of a mini drill. Wounds were sprayed with 10 % lidocaine and the exposed dura mater was protected with a thin layer of petroleum jelly to avoid drying. The prepared animals were wrapped in a warm cloth to maintain body temperature and were put aside for at least 30 min for recovery.

2.2.4.2. Recording and evaluation

For recording, the rat was placed into the stereotaxic frame of the electrophysiological setup. Here, a thermostated (+36.5°C) base plate was used to support the rat's underside during recording. Silver electrodes were placed on the primary somatosensory (SS) visual (VIS) and

auditory (AUD) areas (localized with the aid of the stereotaxic atlas by Zilles, 1984). A stainless steel clamp was attached to the cut skin edge as indifferent electrode.

The biological signals were amplified ($10^4\times$), filtered with 5 Hz and 1 kHz boundaries, fed into the digitizer interface (sampling frequency: 2 kHz for spontaneous and 8 kHz for evoked activity), and stored on PC. The complete recording and evaluation was executed by the software Neurosys 1.11 (Experimetria Ltd, Budapest, Hungary).

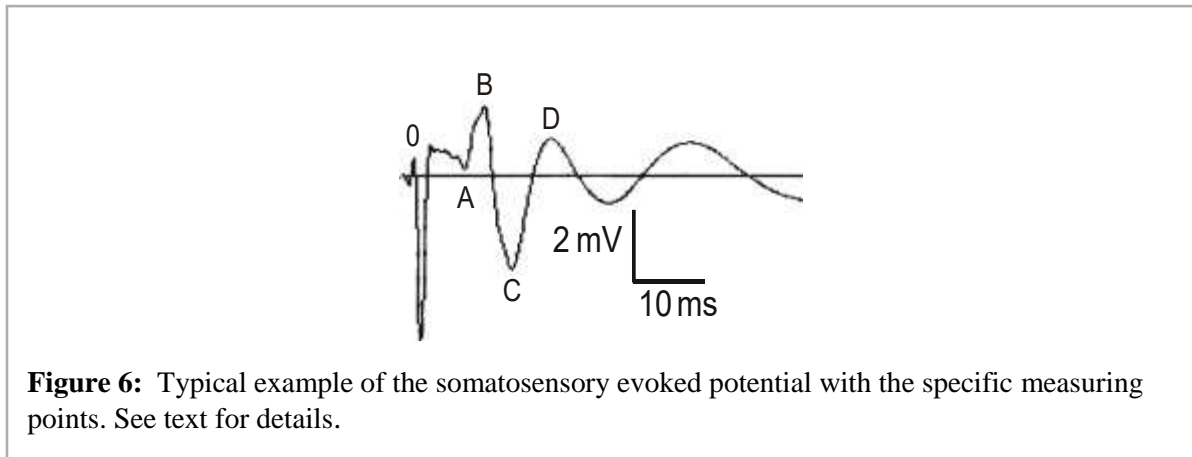
The session started with six minutes recording of spontaneous activity (electrocorticogram, ECoG) from the three sensory cortical areas simultaneously. From the ECoG records, the relative spectral power of the frequency bands: delta, 0.5-4 Hz; theta, 4-7 Hz; alpha, 8-13 Hz; beta1, 13-20 Hz; beta2, 20-30 Hz; gamma, 30-50 Hz (Kandel and Schwartz, 1985) was determined by the software automatically.

Then, evoked potentials (EPs) were recorded from the same cortical sites. All stimuli were of just supramaximal strength (meaning that, e.g., the stimulus voltage was increased until the evoked response reached maximal amplitude and ca. 5% was added) and well above background. Electrical stimulation of the whiskers and the base of tail was done by delivering rectangular electric stimuli (3-4 V, 0.05 ms). The intensity of the visual stimulation was ca. 60 lux, and that of the auditory stimuli, 40 dB (both in 0.2 ms pulses). Trains of 50 stimuli were applied and the evoked potentials (EPs) recorded. The standard frequency of the stimulation was 1 Hz. By varying the frequency of stimulation, dynamic interaction of successive excitation processes in the sensory system can be detected which in turn may reflect the actual state of the CNS (Papp et al., 2004). Hence, frequency dependence in the parameters of the SS EPs was determined by stimulating with 2 and 10 Hz frequency also. Based on the effects on motor behavior seen in the pilot study, the possible effect of nano-TiO₂ treatment on the connection between the motor cortical area and the caudato-putamen was also tested. A steel needle recording electrode was inserted in the CPu (stereotaxic coordinates: AP 0, L3, V -5; Paxinos and Watson, 1982), and the cortex was stimulated bipolarly at AP -1, L 2 with the stimulus trains of 50 described above.

Finally, compound action potentials (CAP) of the tail nerve were recorded. These were evoked by means of a pair of stimulating needle electrodes inserted at the base of tail (delivering similar electric stimuli as used to stimulate the whiskers), and were recorded distally by another pair of needles at a distance of 50 mm.

Evoked activity was automatically averaged off-line, and the parameters were measured manually by means of screen cursors of the software. Exemplified on the SS EP, onset latency was measured between the stimulus artefact (designated 0 in Fig. 7) and onset of the first wave

(A in Fig. 6). Duration of the EP was calculated as the difference of the $0-D$ and $0-A$ times. Onset latency of visual and auditory EPs was measured in the same way. The tail nerve CAP also had biphasic shape. There, onset latency was defined analogously with the $0-A$ distance. Tail nerve conduction velocity was calculated from the onset latency and the distance of the electrodes. From double-pulse stimulation of the tail nerve, relative refractory period was determined.



2.2.5. Chemical and biochemical measurements

2.2.5.1. Ti level measurement

The amount of titanium deposited in the treated cells or in tissues of treated rats was determined by inductively coupled plasma as spectrometry (ICP-MS), a method capable of detecting metals and several non-metals at concentrations as low as one part in 10^{15} (Pröfrock and Prange, 2012). Blood and tissue samples were dried to constant weight at 80°C , and were digested as follows: 3 ml cc. HCl/g wet tissue for 90 min at 90°C , then an equal volume of cc. HNO_3 was added and digested for further 90 min. This procedure was necessary to reliably dissolve all TiO_2 (see paper No. IV in Appendix). The resulting liquid was filtered on 0.45 nm hydrophilic membrane filter and diluted to 100 mL volume. The measurement itself was done at the Department of Inorganic and Analytical Chemistry, University of Szeged Faculty of Science and Informatics. The instrument used was an Agilent Technologies 7700 X ICP-MS, with ORS3 collision cell and Agilent I-AS autosampler (Agilent Technologies, Santa Clara, CA, USA).

2.2.5.2. Measurement of oxidative stress

The frozen tissue samples were powdered with a pestle and mortar in liquid nitrogen. For detection of lipid peroxidation by thiobarbituric acid reactive substances (TBARS) assay (method of Serbinova et al., 1992), and for catalase activity measurement (method of Beers and

Sizer, 1953), 100 µg tissue powder was taken and homogenized in 1 mL PBS by three cycles of freeze-thawing in liquid nitrogen. The lysates were centrifuged at 8000 g for 10 minutes, and the supernatant was used for the measurements. Protein concentrations of the lysates were determined by the method of Bradford (1976).

For lipid peroxidation assessment, malondialdehyde (MDA) was measured as follows: 50 µL lysates were incubated with 450 µL reagent (15% trichloroacetic acid, 0,4% thiobarbituric acid, 0.25 M HCl) for 20 minutes at 100°C. After centrifuging at 2000 g for 5 minutes, absorbance of the supernatant was measured at 532 nm. For assessing catalase activity, 5 µL tissue lysate was mixed with phosphate buffer (50 mM KH₂PO₄, 50 mM Na₂HPO₄) containing 0.1% H₂O₂, and the absorbance was continuously measured at 240 nm for 3 minutes. Using absorption difference/min values, catalase activity was expressed in Bergmeyer units (BU; 1 gram of H₂O₂ degraded enzymatically in 1 minute at 25 °C). The results of TBARS assay and catalase activity were normalized to the protein concentration of the sample.

2.2.5.3. Detection of cytokines

Cytokine profile in the lung tissue samples was determined in a semiquantitative way from tissue homogenates by using the Proteome Profiler Rat Cytokine Array Kit, Panel A (29 rat cytokines and chemokines; Bio-Techne Ltd., R&D Systems, Minneapolis, MI, USA). The factors to be detected by the kit were cytokine-induced neutrophil chemoattractants (CINC-1, -2α/β, -3), ciliary neurotrophic factor (CNTF), fractalkine, granulocyte-macrophage colony-stimulating factor (GM-CSF), soluble intercellular adhesion molecule-1 (sICAM-1), interferon gamma (IFN γ), interleukins (IL-1α, -1β, -1ra, -2, -3, -4, -6, -10, -13, -17), IFN γ induced protein (IP-10), lipopolysaccharide induced CXC chemokine (LIX), L-selectin, IFN γ induced monokine MIG), macrophage inflammatory proteins (MIP-1α, -3α), chemokine (C-C motif) ligand 5 (CCL5), TIMP metalloproteinase inhibitor 1 (TIMP-1), tumor necrosis factor alpha (TNF-α), and vascular endothelial growth factor (VEGF).

Of each rat's powdered lung tissue, 20 mg was taken and lumped together group by group to collective samples of 200 mg, and were homogenized in a PBS containing protease inhibitor cocktail (Roche, Basel, Switzerland) and 1% Triton-X-100. After three freeze-thaw cycles using liquid nitrogen, cellular debris was removed by centrifugation at 10,000 g for 5 minutes. Protein concentration of the supernatant was measured using the Bradford reagent, and a quantity corresponding to 400 µg protein was brought to the array from each sample. Cytokines in the samples were determined by an ELISA-based procedure. The membranes were developed

using the Chemi Reagent Mix (Immobilion, Merck, Darmstadt, Germany) and the chemiluminescent signal was detected by the C-DiGit Blot Scanner (LI-COR, Lincoln, NE, USA).

2.3. Experimental design: *in vitro* work

In vitro work was done on A549 cells. This lung alveolar adenocarcinoma cell line (Lieber et al., 1976) was purchased from ATCC. Cell culturing and the corresponding biochemical work was done at the Department of Biochemistry and Molecular Biology, University of Szeged Faculty of Science and Informatics.

2.3.1. Culturing of the cells and exposure to nano-TiO₂

The cells were maintained in low glucose (1 g/L) Dulbecco's minimal essential medium, complemented with 10% fetal bovine serum, 2 mM L-glutamine, 0.01% streptomycin and 0.005% ampicillin, and cultured under standard conditions in a 37°C incubator containing 5% CO₂ in 95% humidity.

For the tests applied, the cells were grown for 24 hours in multi-well plates and then treated with the TiO₂ nanosuspension.

2.3.2. Biochemical investigations

The three biochemical measurements listed below were repeated three times, using at least 4 (MTT, DCFDA) or 2 (apoptosis) biological replicates.

2.3.2.1. Cell viability test

To estimate the effect of TiO₂ NPs (and of PAA used in the vehicle) on the viability of the cells, 10⁴ cells/well were seeded into 96 well plates and grown as described above. After 24 hours, TiO₂ NPs were applied in concentrations ranging from 0.025 to 2.00 mg/mL in the medium. To cells in separate wells, the corresponding amount of PAA was added. After further 24, 48 or 72 hours, the NP- or PAA-containing medium was removed and the cells were incubated with 0.5 mg/mL yellow MTT (3-(4,5-dimethylthiazolyl-2)-2,5-diphenyltetrazolium bromide) (SERVA Electrophoresis GmbH, Heidelberg, Germany) diluted in culture medium for 1 h in 37°C. The generated formazan crystals were solubilized in dimethyl sulfoxide and the absorbance at 570 nm was determined using a Synergy HTX plate reader (BioTek Germany, Bad Friedrichshall, Germany).

3.2.2. Detection of reactive oxygen species

The cells were cultured as above for one day, and then treated with TiO₂ NPs or PAA for 48 hours, as described above. After these treatments, the cells were washed with PBS and were incubated with 10 μM DCFDA (2',7'-dichlorofluorescein diacetate) solution for 1 h. Fluorescence intensity was measured by Synergy HTX plate reader.

2.3.2.3. Apoptosis detection

For this test, $3 \cdot 10^5$ A549 cells were seeded into 6-well plates and grown for 24 hours. On the following day, the cells were exposed to 0.1 mg/mL TiO₂ NPs or to PAA in the corresponding concentration. According to the method published by Rieger et al. (2011), the cells after 24, 48 and 72 hours of treatment were stained with Alexa488-conjugated AnnexinV and with propidium iodide (Thermo Fisher Scientific, Waltham, MA, USA). Fluorescence intensity was determined using a FACScalibur flow cytometer (BD Biosciences, Erembodegem, Belgium) by measuring 10.000 cells, and the FACS data were analyzed by FlowJo V10 software.

2.4. Pathomorphological investigations

2.4.1. Light microscopic observations

Formalin-fixed lung, hilar lymph node, and kidney tissues were dehydrated and embedded in paraffin using the standard technique. Sections of 3 μm were stained with hematoxylin and eosin (HE). The stained sections were observed under 10x magnification, and images were taken and stored using standard digital microphotography. A Zeiss Imager.Z1 microscope was used with a Zeiss Axiocam506 color digital camera (Carl Zeiss Technika Kft., Budaörs, Hungary).

Quantitative evaluation of the images of HE stained lung and kidney tissue sections was done by means of the ImageJ software (Schneider et al., 2012). After calibrating and validating the system, objects of interest, i.e. macrophages with phagocytosed TiO₂ NPs, were manually marked on the digitized light microscopic image, and the software calculated their number, total area and typical maximal diameter.

2.4.2. Scanning Electron Microscopic (SEM) examinations

To observe the interaction of A549 cells with the TiO₂ NPs, $3 \cdot 10^5$ cells were seeded onto plastic cover slips placed in 6-well plates, and were grown for one day, then exposed to 0.1 mg/mL TiO₂ NPs for 24 hours. The cells were washed and fixed using 2.5% glutaraldehyde (dissolved in

modified Sørensen buffer, pH 7.6). The samples were dehydrated in an ascending ethanol series, followed by a series of tert-butanol:ethanol mixture at room temperature, then incubated in tert-butanol overnight at 4°C and finally lyophilized. The slips were mounted on specimen stubs using electrically conductive double-sided adhesive tape and a 4-5 nm gold-palladium coating was applied to decrease charging artefacts and radiation damage of the sample. SEM imaging was performed by a Hitachi S4700 electron microscope (Hitachi High-Technologies Europe GmbH, Krefeld, Germany) using 10 kV accelerating voltage and 10 µA emission current. To prove the presence of Ti, EDS measurements were carried out with a Röntec QX2 EDS detector installed on the SEM at 20 kV and 10 µA.

2.4.3. Transmission Electron Microscopic (TEM) observations

To detect intracellular accumulation of TiO₂ NPs in A549 cells, 10⁵ cells were seeded onto 0.4 µm pore polyester membrane inserts (Corning Hungary, Budapest, Hungary), were cultured and exposed as above, then washed in PBS and fixed in 4% glutaraldehyde diluted in PBS for 2 hours, and finally embedded in gelatin (2% in PBS). The obtained specimen was sliced to 1-2 mm cubes, which were re-embedded in epoxy by a routine TEM sample preparation protocol. Semi-thin sections of 1 µm were prepared to identify the cell monolayer, the blocks were trimmed, and thin sections of 70 nm were obtained and stained with uranyl and lead solutions.

To detect the NPs in treated rats' lungs and kidneys, the samples described in 2.4.1. were re-embedded in epoxy, then 70 nm thick sections were cut, stained as above, and placed on oval slot copper grids. Images were captured by a Jeol 1400 plus 120 kV using 100 kV voltage.

2.5. Preliminary experimentation

The design of the *in vivo* experiment presented here was largely based on two previous ones (see papers No. III and IV in Appendix), regarded in this context as a pilot study. These were done on rats of the same strain and age range, and the neuro-functional tests applied were also largely (cognitive behavioral tests) or nearly completely (electrophysiology) identical. In those experiments, TiO₂ NPs of three kinds: spheres of ca. 10 nm diameter, spheres of ca. 100 nm diameter, as well as nanorods identical to the ones in main experiment detailed above (2.2 to 2.4.) were applied.

The main outcomes of the pilot study were as follows:

- The model system as a whole (animals, test substances, way of application) is suitable.

- Functional alterations of the nervous system on action of nano-TiO₂ are detectable at the level of behavioral and electrophysiological phenomena.
- The spectrum of behavioral test methods should be broadened;
- It is crucial to obtain a sufficiently stable suspension of the TiO₂ NPs.

Based on this, the nanorods were chosen for the main experiment, also because the majority of available papers on toxicity on nano-TiO₂ dealt with spherical particles. Further, it was decided to examine the fate and effects of the NPs in a more comprehensive way from entry in the rats' organism to the possible excretion.

2.6. Data analysis

From the individual rats' data, group mean and standard deviation was obtained. Depending on the normality of data distribution, checked by Shapiro-Wilk test. Body/organ weight, as well as behavioral and histopathological data, with sufficiently normal distribution, were analyzed by one-way ANOVA and post hoc Tukey test, while for electrophysiological and chemical-biochemical data nonparametric Kruskal-Wallis ANOVA and post hoc Mann-Whitney U-test was used. Changes of activity in the OF test, repeated three times during the experimental period, were tested by repeated measures ANOVA and post hoc Tukey test. The limit of significance was $p < 0.05$ for all measurements.

The software used was SPSS version 23.0 (IBM Corp., USA).

The possible linear correlation between data sets was tested by the "linear fit" function of MS Excel. This function uses the least squares method to fit a straight line to the measurement data, and examines the strength of relationship with Fisher's F test

3. RESULTS

3.1. Summary of the findings of the pilot study

The results of the two preliminary experiments are summed up in Table 2. As one can see, the effects observed were not fully unequivocal and conclusive. They indicated that the basic approach of the research work was sound but also that amendments in the methodology were necessary.

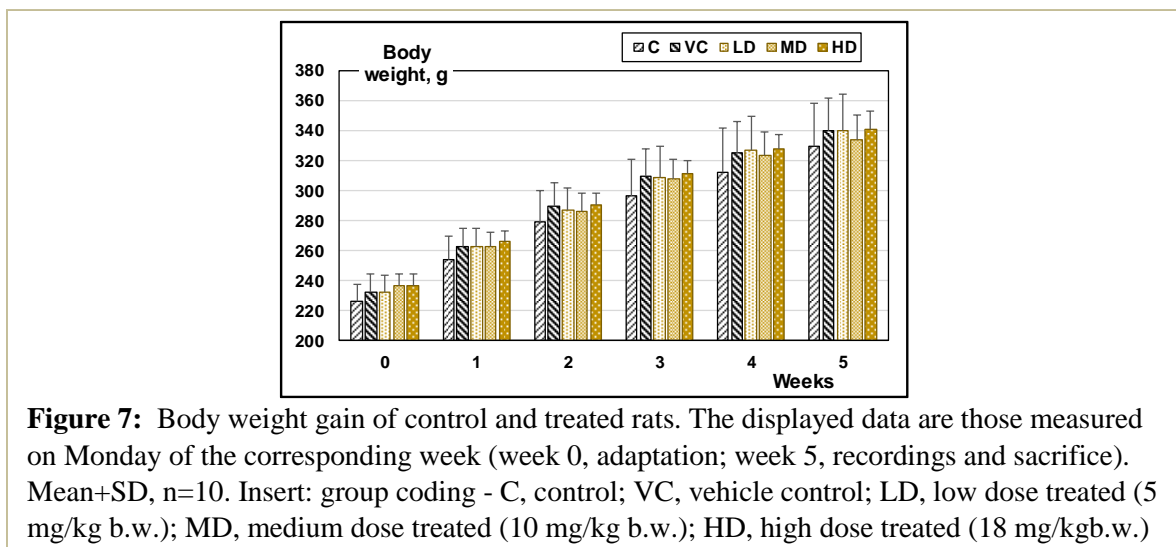
Table 2: Changes in the investigated parameters of the rats in the pilot study.

Investigations	Difference, treated vs. control	
	Pre-experiment 1	Pre-experiment 2
Body weight gain	↓ (with anomalous dose dependence)	no significant effect
Organ rel. weights	lung, kidney ↑	lung ↑
Ti levels	lung ↑↑, brain ↑	lung ↑↑, brain ↑
Oxidative stress, TBARS	↑	no significant effect
Open field	corner dwell time ↑	corner dwell time ↑
Climb test	not done	↓
EP latencies	↑	↑
Nerve conduction velocity	↓	↓

The arrows show the direction and extent of changes.

3.2. Main experiment – General toxicity in vivo: effects on body and organ weights

Similar to what was seen in Pre-experiment 2, treating the rats with the rod-shaped TiO₂ NPs resulted in no significant difference in body weight gain and final body weight (Fig. 7).



Among the relative organ weights, significant difference between the groups *HD* vs. *C* and *VC* was found in case of the lungs and kidneys (Table 3) while the difference in the lower dose groups remained below significance. Lung relative weight was different between groups *C* and *VC*, suggesting an own, mild, effect of the vehicle, but this did not influence the significance of the *HD* vs. *VC* difference. Brain samples showed no noteworthy change of relative weight.

Table 3: Organ weights related to 1/100 body weight in the control and treated animals.

Groups	Lungs	Kidney (right)	Kidney (left)	Brain hemisphere (right)	Cerebellum
<i>C</i>	0.519±0.198	0.393±0.096	0.380±0.081	0.502±0.054	0.094±0.010
<i>VC</i>	0.607±0.256	0.355±0.046	0.348±0.041	0.498±0.037	0.091±0.006
<i>LD</i>	0.687±0.148	0.402±0.070	0.402±0.068	0.501±0.027	0.095±0.008
<i>MD</i>	0.755±0.235	0.394±0.047	0.399±0.064	0.498±0.027	0.091±0.008
<i>HD</i>	0.863±0.105**##	0.468±0.051##	0.459±0.047**##	0.497±0.025	0.090±0.006

Mean±SD; n=10. **: p< 0.01 vs. *C*; ##: p<0.01 vs. *VC* (one-way ANOVA)

3.3. Effects of the TiO₂ nanorods on the rats' lungs and on lung-derived cells

The toxic effects on the lungs, suggested by the significant change of relative organ weight, were examined using a complex, morphological-chemical-biochemical, approach.

3.3.1. Presence of TiO₂ NPs in the lung tissue

The toxic effect of nano-TiO₂ treatment on the lungs, manifested in the relative organ weight (see Table 3), was paralleled by detectable deposition of Ti in the treated rats' lungs. ICP-MS measurements revealed massive increase of metal level in the lung samples (Table 4). In the same animals, increase of the blood Ti level was much weaker and remained below significance.

Ti in the lung tissue retained its NP form, at least partially. HE-stained histological sections of the lungs and hilar lymph nodes showed macrophages laden with dark particles (Fig. 8). Quantification of the macrophages in the light microscopic images using ImageJ (Table 4) revealed a highly significant and dose-dependent difference in their number and size. TEM images, showing NPs and their conglomerates of several hundred nm located within

multivesicular bodies in lung macrophages (Fig. 9) were in line with that. These observations suggested that macrophages might be involved in the systemic spread of the NPs delivered to the lungs – all the more that other possible ways of access to systemic circulation, such as NPs within epithelial cells or free in the interstitium, were not observed. It was also of note that alveolar area decreased and interstitial area increased in the *LD* and *HD* rats' sections.

Table 4: Tissue metal levels in the control and treated rats' lung and blood samples, and image analysis results of the lung light microscopic sections.

Groups	Tissue Ti levels (mg/kg bw)		ImageJ results (n=10/group)		
	<i>In the lungs</i> n=10/group	<i>In blood</i> n=8/group	<i>Number of</i> <i>macrophages /</i> <i>image</i>	<i>Maximal</i> <i>diameter</i>	<i>Area</i>
<i>C</i>	10671.81 ± 12808.42	153.34 ± 314.41	n.d.	n.d.	n.d.
<i>VC</i>	7804.64 ± 7397.54	205.65 ± 387.07	n.d.	n.d.	n.d.
<i>LD</i>	304768.22 ± 331486.69***#	1077.10 ± 1672.47	179	34.90 ± 2.59***##	725.82 ± 116.85***##
<i>MD</i>	305732.52 ± 224966.61***#	1109.23 ± 893.51	192	40.70 ± 3.48***##	1055.16 ± 185.22***##
<i>HD</i>	772751.12 ± 491495.15***#	1182.69 ± 1887.36	265	43.00 ± 2.88***##°	1196.57 ± 168.77***##°°

Mean±SD, n= as indicated.

, *: p<0.01, 0.001 vs. *C*; #, ##: p<0.01, 0.001 vs. *VC*; °, °°: p<0.05, 0.01 *HD* vs. *LD* (one-way ANOVA).

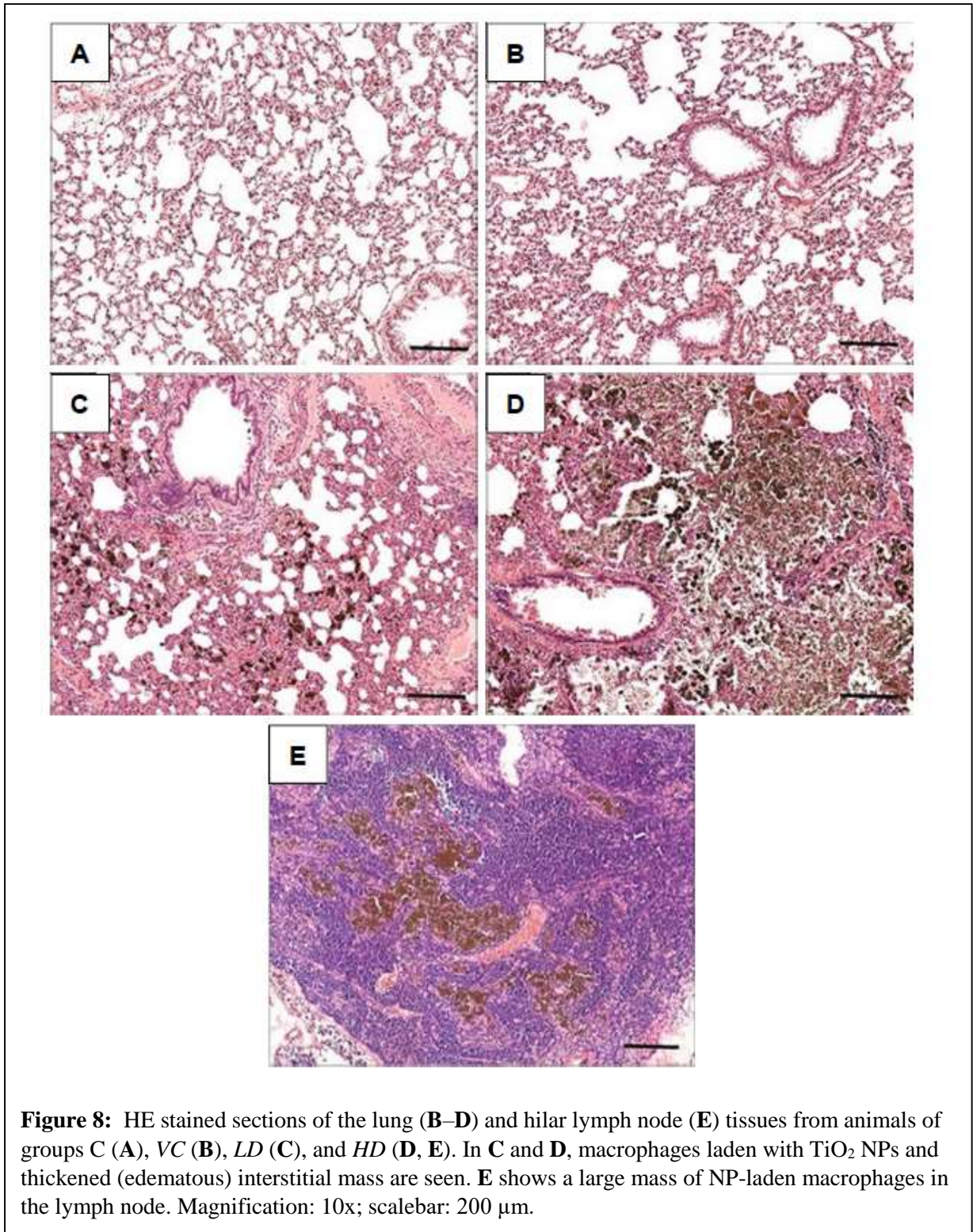
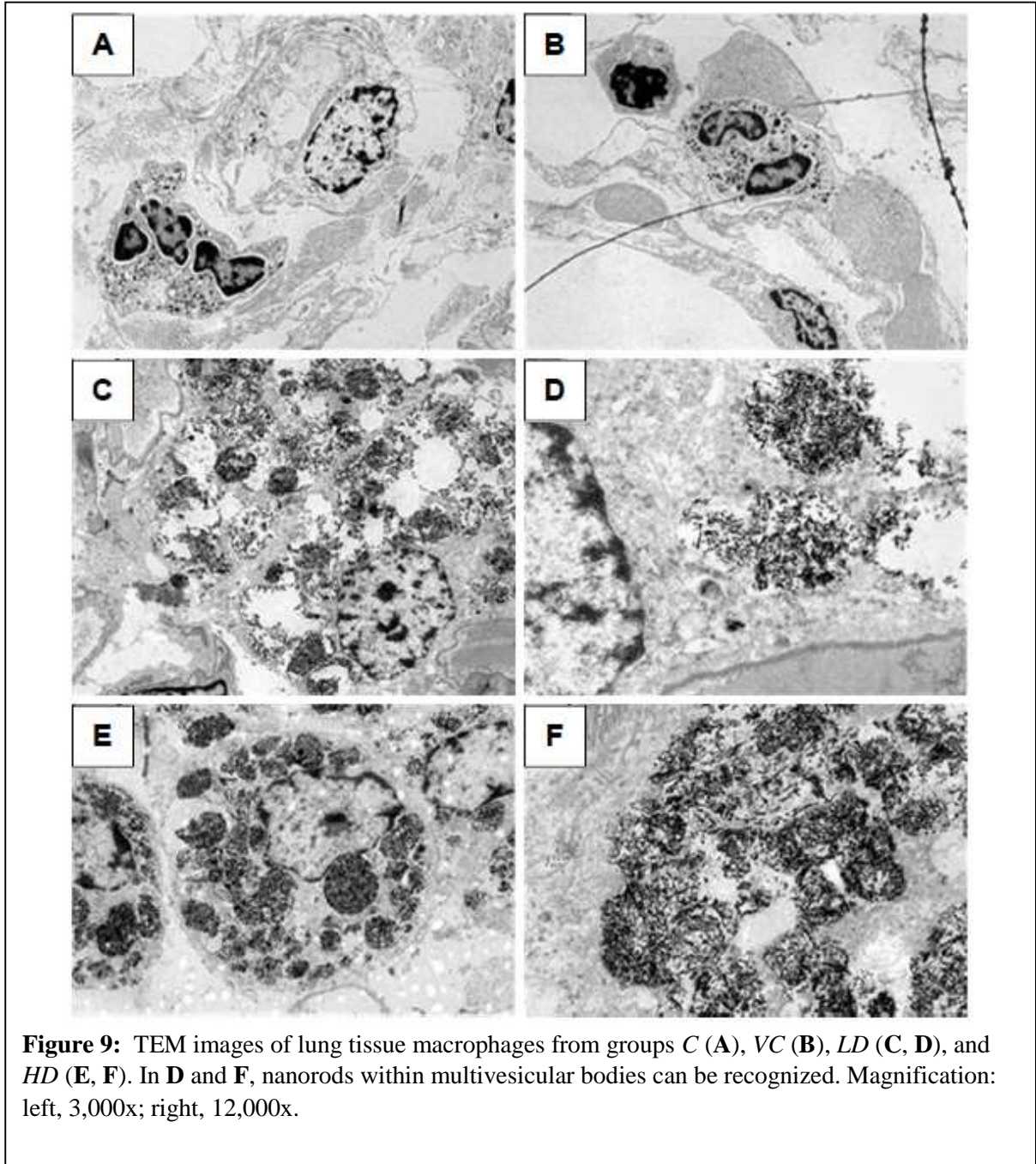


Figure 8: HE stained sections of the lung (**B–D**) and hilar lymph node (**E**) tissues from animals of groups C (**A**), VC (**B**), LD (**C**), and HD (**D, E**). In **C** and **D**, macrophages laden with TiO₂ NPs and thickened (edematous) interstitial mass are seen. **E** shows a large mass of NP-laden macrophages in the lymph node. Magnification: 10x; scalebar: 200 μm.



3.3.2. Biochemical indicators of toxicity of the TiO_2 nanorods present in the lung tissue

The presence of nano- TiO_2 in the lung tissue of the treated rats resulted in overproduction of ROS and generation of oxidative stress. The level of MDA (indicator of lipid peroxidation) increased significantly in the *HD* group only, while catalase activity was significantly raised in *MD* and *HD* (Table 5). PAA alone (group *VC*) had no effect on these oxidative stress parameters despite its effect on lung weight (cf. Table 3).

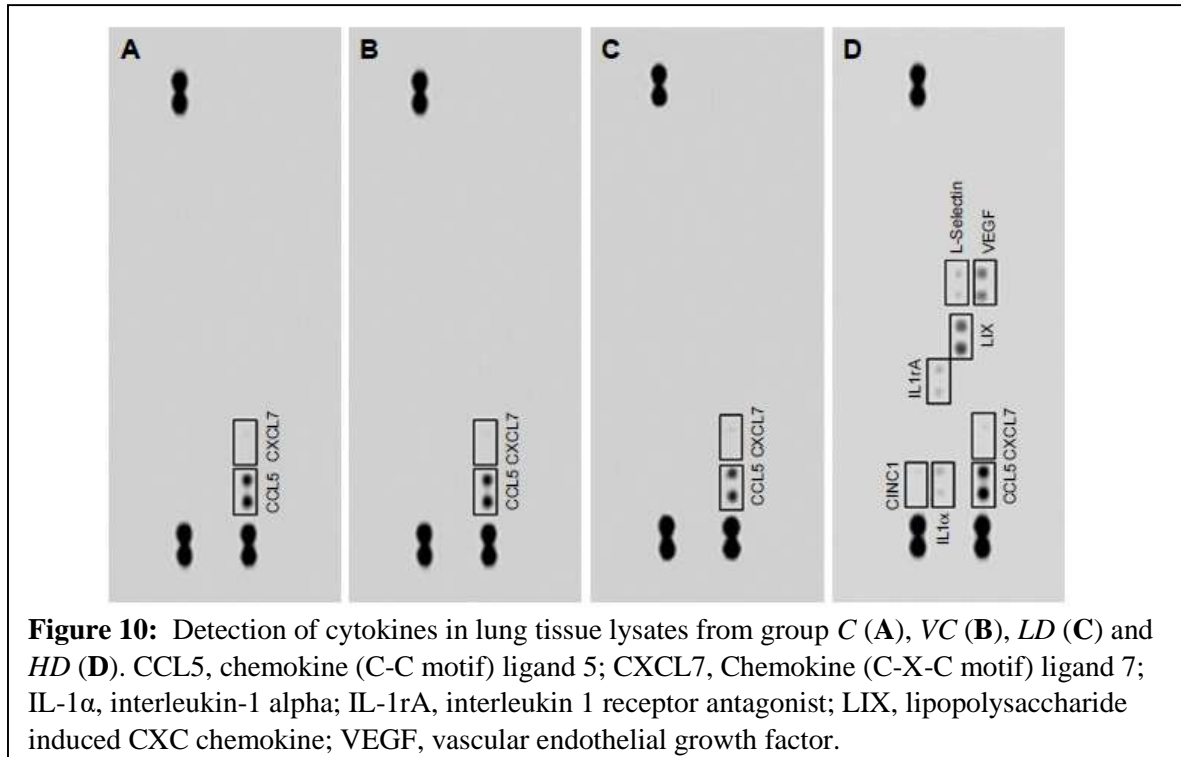
Table 5: Indicators of oxidative stress in the control and treated rats' lung samples.

Groups	TBARS ($\mu\text{M MDA/mg protein}$)	Catalase activity (BU/mg protein)
<i>C</i>	1.0389 ± 0.3149	0.00238 ± 0.00034
<i>VC</i>	1.0783 ± 0.3325	0.00214 ± 0.00049
<i>LD</i>	1.0250 ± 0.3855	0.00212 ± 0.00095
<i>MD</i>	0.9868 ± 0.3374	$0.00334 \pm 0.00078^{***\#\#}$
<i>HD</i>	$1.2985 \pm 0.3890^*$	$0.00345 \pm 0.00105^{***\#\#}$

Mean \pm SD, n=10.

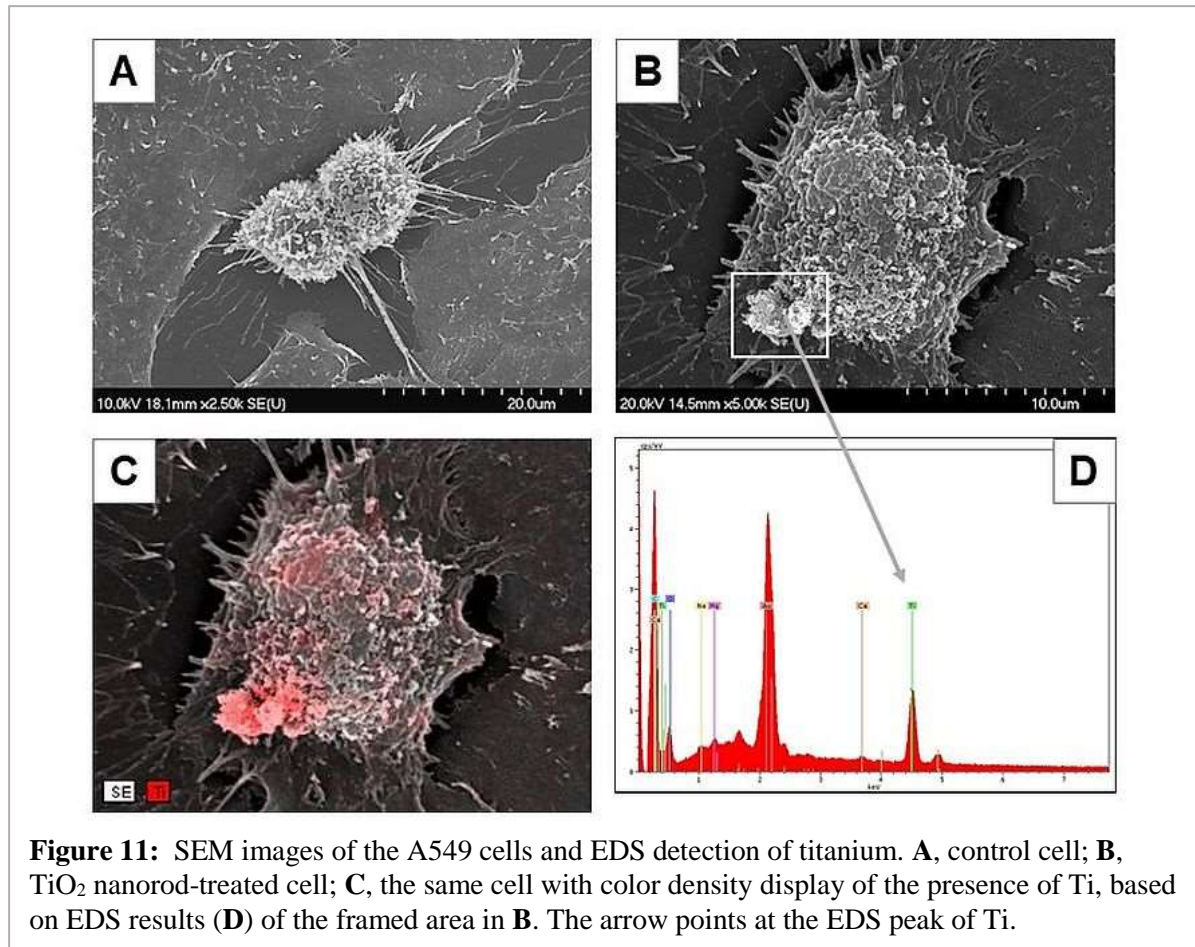
*, **: p<0.05, 0.01 vs. *C*; #: p<0.01 vs. *VT* (one-way ANOVA)

The action of TiO₂ nanorods on the lung cells resulted in massive activation of various cytokines as well, especially in group *HD*. The cytokine profile in this group demonstrated expression of several proteins not present in the controls and lower dose groups (Fig. 10). Several of the cytokines, e.g. IL-1 α and CINC-1, belong to acute inflammation and phagocyte recruitment, whereas VEGF was indicative of the inflammation becoming chronic.



3.3.3. Presence and toxicity of TiO₂ NPs in lung-derived cells in vitro

TiO₂ nanorods were observed on the surface of the treated A549 cells by SEM. In Fig 11B, the cluster of white particles at the lower left region of the cell appeared to be nano-TiO₂. EDS analysis proved the presence of Ti in the visualized NPs (Fig 11C,D). In C, nanorods in the region with lower red density (false-color indication of presence of Ti) were probably attached to the plasma membrane, while where red density was maximal, they might have been already internalized.



TEM images of cells after 24-hour treatment with 0.1 mg/mL dose confirmed that TiO₂ nanorods were internalized (Fig. 12). Intracellularly, the nanorods were localized mainly in electron dense endosomes, in membrane coated multilamellar and multivesicular bodies, but not within mitochondria and nuclei.

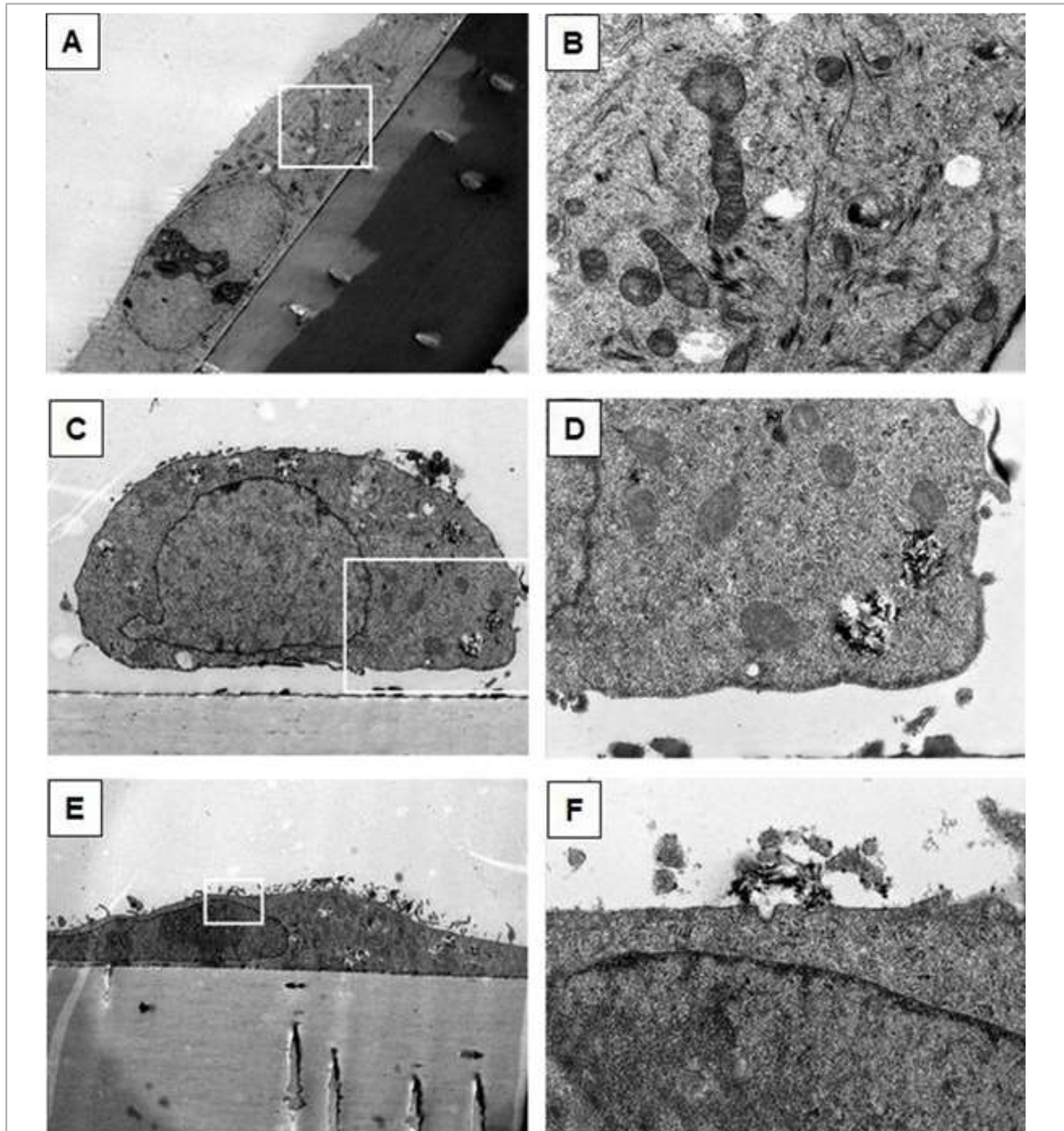


Figure 12: Internalization of the TiO₂ nanorods by the A549 cells. **A**, control cell (1,500x) with intact organelles (**B**, 10,000x); **C**, treated cell (4,000x) with internalized NPs in multivesicular bodies (**D**, 12,000x); **E**, another treated cell (2,000x) with a caveola being formed on the cell surface near a cluster of NPs (**F**, 20,000x). White frames in **A**, **C** and **E** show the cut-outs magnified in **B**, **D** and **F**.

Exposure of the A549 cells to TiO₂ nanorods caused dose- and time-dependent viability loss. PAA itself exhibited some effect on cell viability, but TiO₂ nanorods were significantly more toxic compared to the stabilizing agent (Fig. 13A) and the presence of ROS in the treated A549 culture increased at least twofold vs. PAA treated cells (Fig. 13B). Viability levels after 24 and 48 hours demonstrated time dependent development of cytotoxicity.

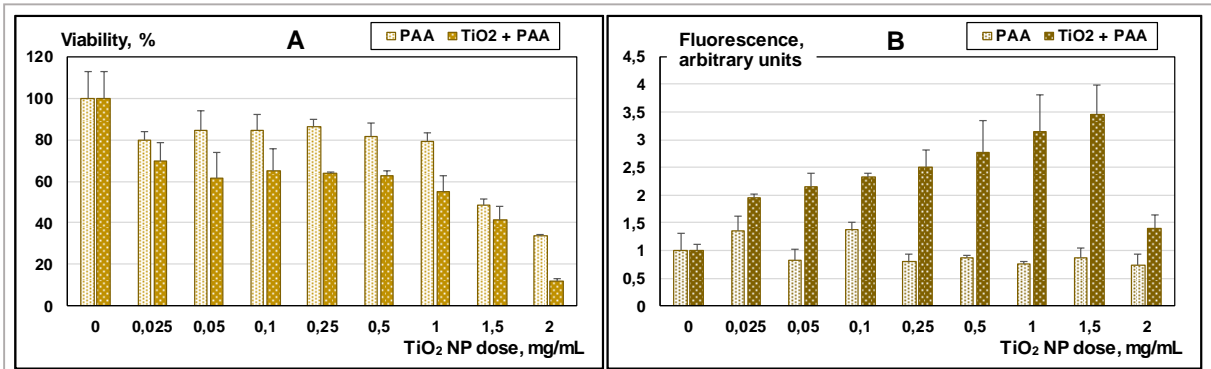


Figure 13: Effects of TiO₂ nanorods on A549 cells after 48 hours of exposure. **A**, viability; **B**, free radical generation. Mean+SD, n=3

3.4. Toxicity of the TiO₂ nanorods on the rats' nervous system

3.4.1. Behavioral effects

3.4.1.1. Climb test

Climb test, detecting changes in the rats' motor performance, showed that the 6th/0th week ratio of time-to-fall was lower – in group *HD* significantly lower – in treated rats than in the rats without TiO₂ nanorod exposure, indicating decreased muscle force and/or coordination (Fig. 14).

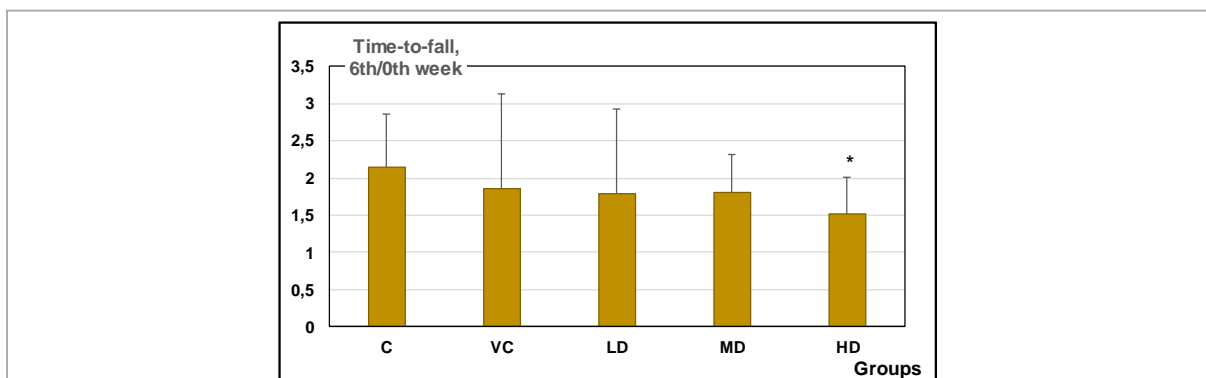


Figure 14: Ratio of time-to-fall in the 6th and 0th week in the control and treated rats. Mean+SD, n= 10. *: p<0.05 vs. C (One-way ANOVA).

3.4.1.2. Elevated plus maze test

EPM test proved to be sensitive in detecting the effect of nano-TiO₂ exposure that appeared to be increased anxiety. Treated rats were significantly less likely to visit the open arms of the maze and stay there (Fig. 15). Moreover, their stay time at the end of the open arms was practically zero whereas in both control groups this parameter had a low but positive value (not shown).

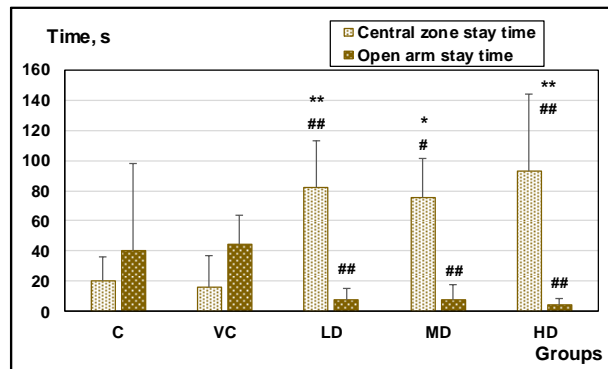


Figure 15: Time spent by the control and treated rats in various parts of the elevated plus maze. Mean±SD, n=8.

*, **: $p > 0.05, 0.01$ vs. C; #, ##: $p < 0.05, 0.01$ vs. VC (one-way ANOVA).

3.4.1.3. Open field test

The rats treated with nano-TiO₂ showed some preference to stay in the corners of the OF box. As seen in Fig. 16, a dose-dependent trend was clearly present but mostly failed to reach significance.

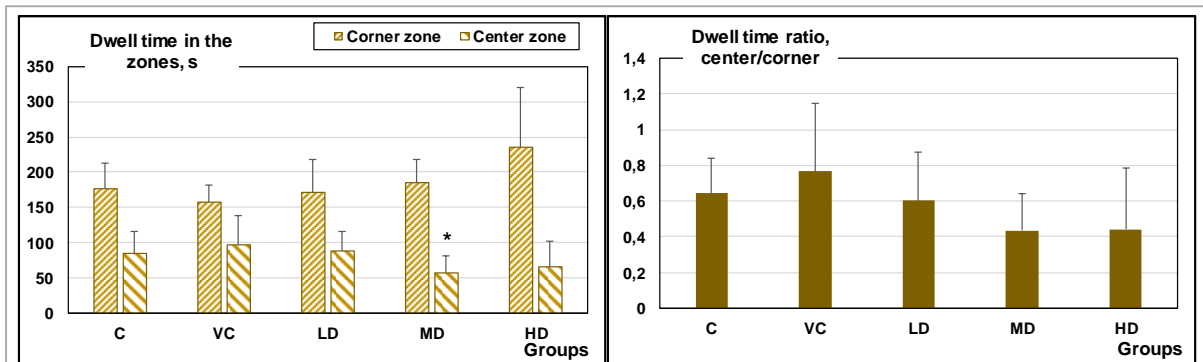
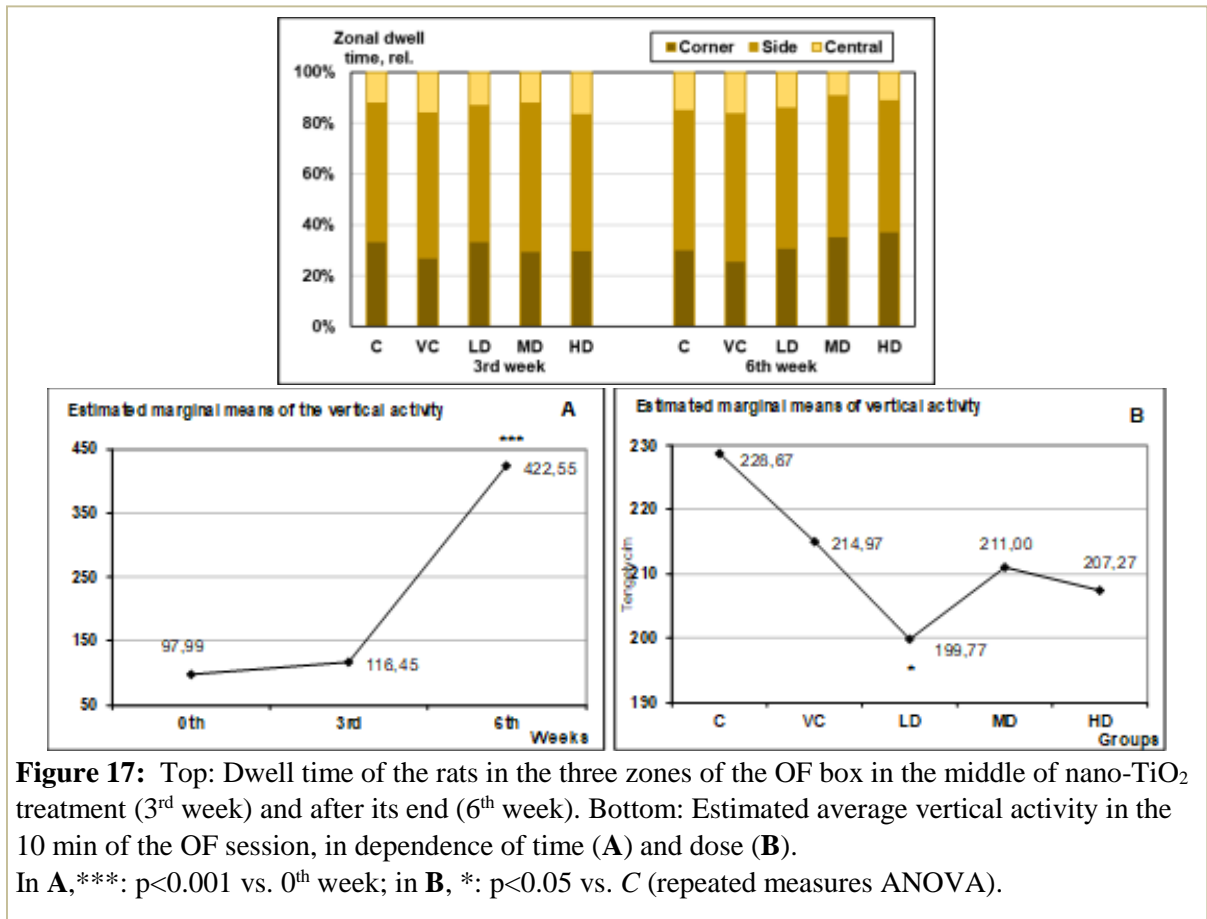


Figure 16: Time spent by the control and treated rats in the central and corner zones of the open field box, and the calculated center/corner ratio.

Mean±SD, n=10. *: $p < 0.05$ vs. C (non-parametric ANOVA)

Fig. 17 shows that the treated rats' preference to the corner zones, indicating increased anxiety, developed mostly in the second half of the treatment period, and was dose-dependent. In the controls, no noteworthy change was seen during the same period. By examining time- and dose-dependence of OF vertical activity together, using repeated-measure ANOVA, it was found that the effect of treatment time (3rd and 6th week) was highly significant ($p=0.000$), effect of dose alone was marginally significant ($p=0.057$). However, no significant interaction was found between the treatment time and the doses. The lower panels in Fig. 17 show that most of the increase of vertical activity happened from the 3rd week on, but also that this increase was less in the treated groups, and in group *LD*, significantly less ($p=0.034$). Consequently, the treated rats' habituation of locomotor activity (a phenomenon that can be used to assess memory in rats) was dose- and time-dependently affected.



3.4.1.4. Acoustic startle response and sensorimotor gating

ASR test at the end of treatment revealed a delay in the latency of the noise-positive response in the treated rat groups but this was significant only in *LD* vs. *C* (despite the clear trend, due to higher SD in the other treated groups; Fig. 18A). Other parameters showed no clear trend. Noteworthy effects of the pre-pulse were seen on the time-to-peak and peak amplitude, suggesting disruption of pre-pulse inhibition, but without clear significance or dose-dependent trend (Fig. 18B).

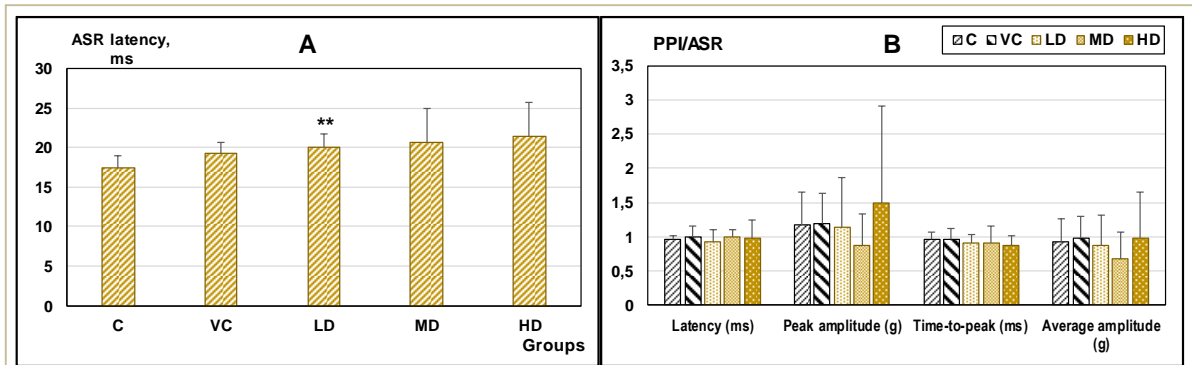


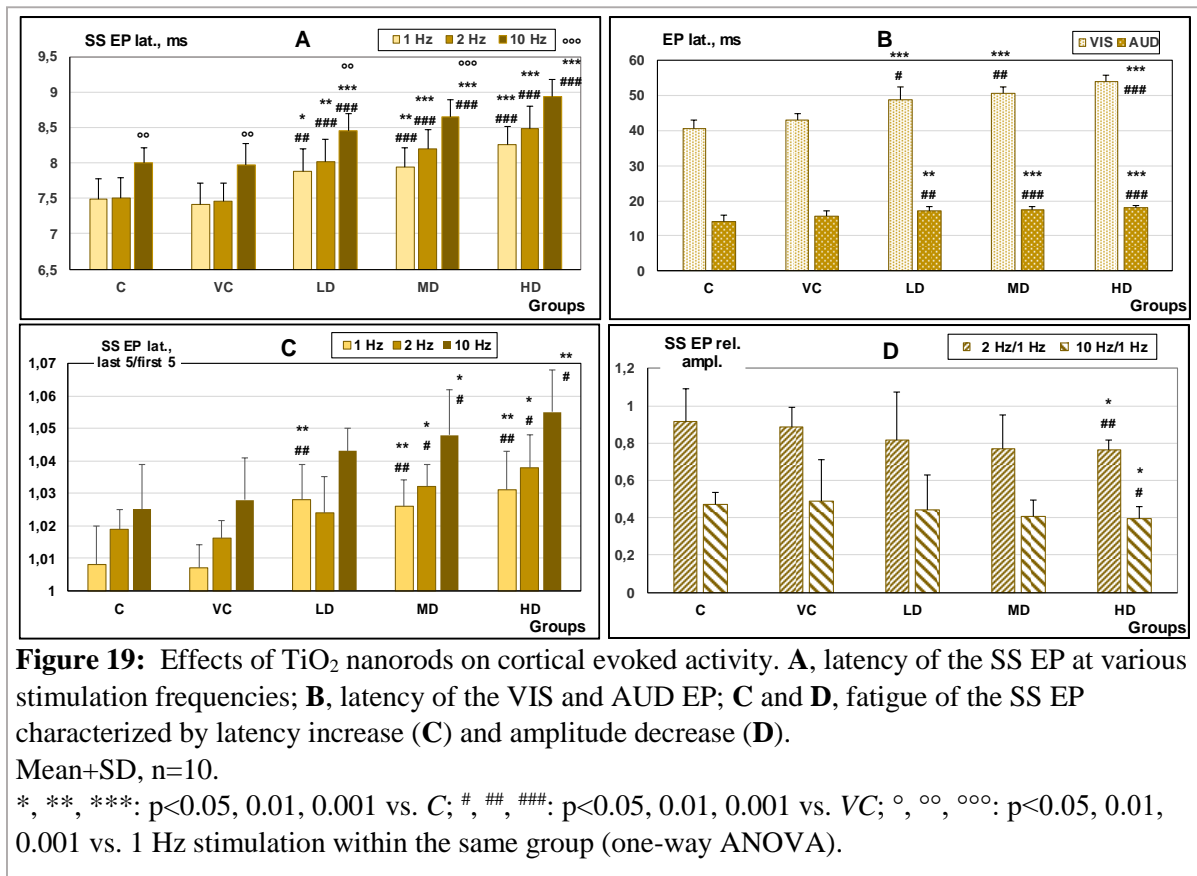
Figure 18: Results of the acoustic startle response test in control and treated rats at the end of treatment. **A**, response latency without pre-pulse; **B**, effect of acoustic startle on the sensorimotor gating.

Mean+SD, n=10. **: $p < 0.01$ vs. *C*.

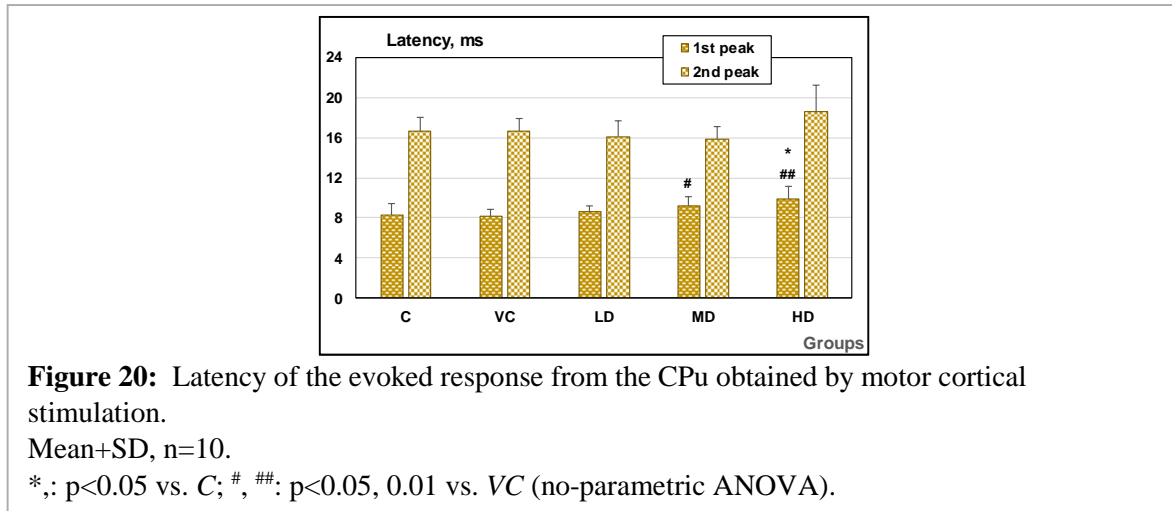
3.4.2. Electrophysiological effects

3.4.2.1. Evoked cortical and subcortical activities

The most characteristic effect was seen on the latency of cortical EPs. Latency lengthening was present in all three modalities (Fig. 19) together with a mild increase of the frequency-dependent lengthening of SS EP latency. In that modality, amplitude of the EPs was also analyzed, and the result was that the average EP amplitude in the series of 50 stimuli showed dose-dependently stronger decrease with increasing stimulation frequency (2 or 10 Hz instead of 1 Hz) in the treated than in the control rats.

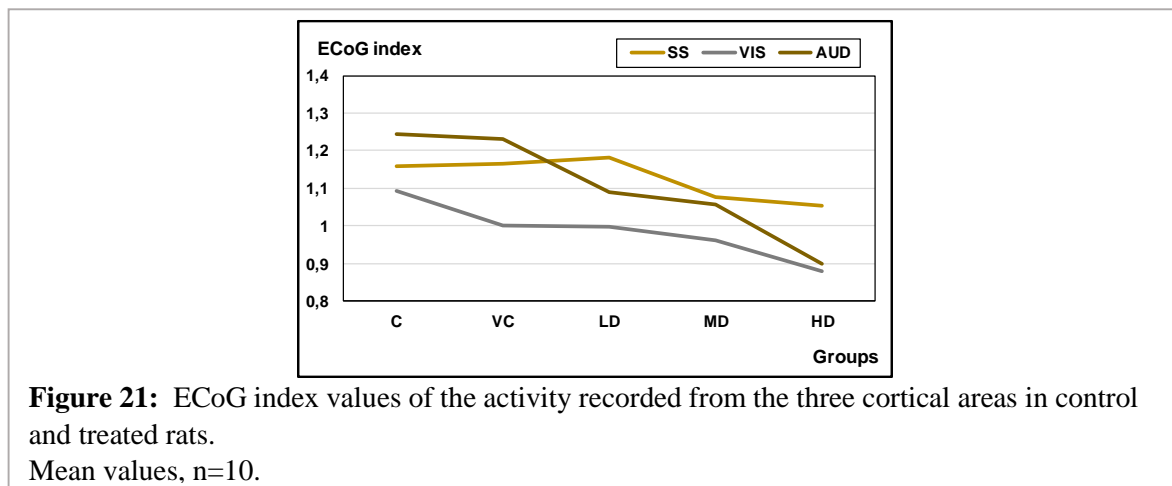


The response recorded from the CPu on stimulating the motor cortex was also slower (had lengthened latency) in the treated rats (Fig. 20).



3.4.2.2. Spontaneous cortical activity

The changes in the frequency spectrum of the spontaneous cortical activity showed a uniform trend in the three recorded areas but were not significant. As seen in Fig. 21, nano-TiO₂ exposure caused a shift in the ECoG index $\left(\frac{[\delta+\theta]}{[\beta_1+\beta_2]}\right)$ ratio) corresponding to increased high frequency and/or decreased low frequency activity in all three cortical areas.



3.4.2.3. Changes in the tail nerve action potential

The recorded CAP from control and treated rats revealed a significant effect of nano-TiO₂ exposure. Conduction velocity decreased and the relative refractory period increased (Fig. 22A) and both effects were dose-dependent. Fig 22B shows that the frequency-dependent decrease of conduction velocity increased in the treated groups, indicating, in unison with the refractory period, that in TiO₂-exposed rats the ability of the nerve to follow frequent stimulation was impaired.

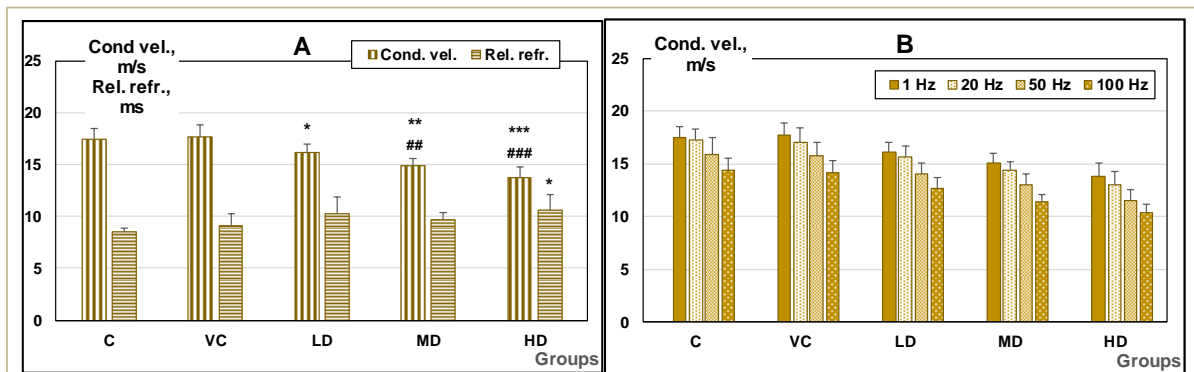


Figure 22: Effects of TiO₂ nanorods on the tail nerve. **A**, conduction velocity and relative refractory period in control and treated rats; **B**, frequency dependence of the conduction velocity. Mean±SD, n=10.

*, **, ***: p<0.05, 0.01, 0.001 vs. C; #, ##, ###: p<0.01, 0.001 vs. VC (no-parametric ANOVA).

3.4.3. Titanium levels in samples of the brain

A tendency of increasing Ti levels in the treated brain samples vs. controls was seen (Table 6) but clear, dose-related and significant change was present only in the cerebellum.

Table 6: Ti levels (µg/kg) in blood and nervous system samples.

Groups	Blood	Brain hemisphere (right)	Cerebellum
C	153.34±314.41	3720.53±2174.79	3303.25±1575.55
VC	205.65±387.07	4044.17±2101.04	4449.27±1262.94
LD	1077.10±1672.47	4265.97±2235.55	6299.95±1971.59**
MD	1109.23±893.51	5514.28±1550.33	5539.96±2593.87***
HD	1182.69±1887.36	5771.13±3090.72	6780.21±1959.08**

Mean±SD; n=10. **, ***: p<0.01, 0.001 vs. C (non-parametric ANOVA)

All the same, diagrams of correlation between electrophysiological and behavioral indicators of neuro-functional damage and tissue Ti levels suggested causal relationship (Fig. 23).

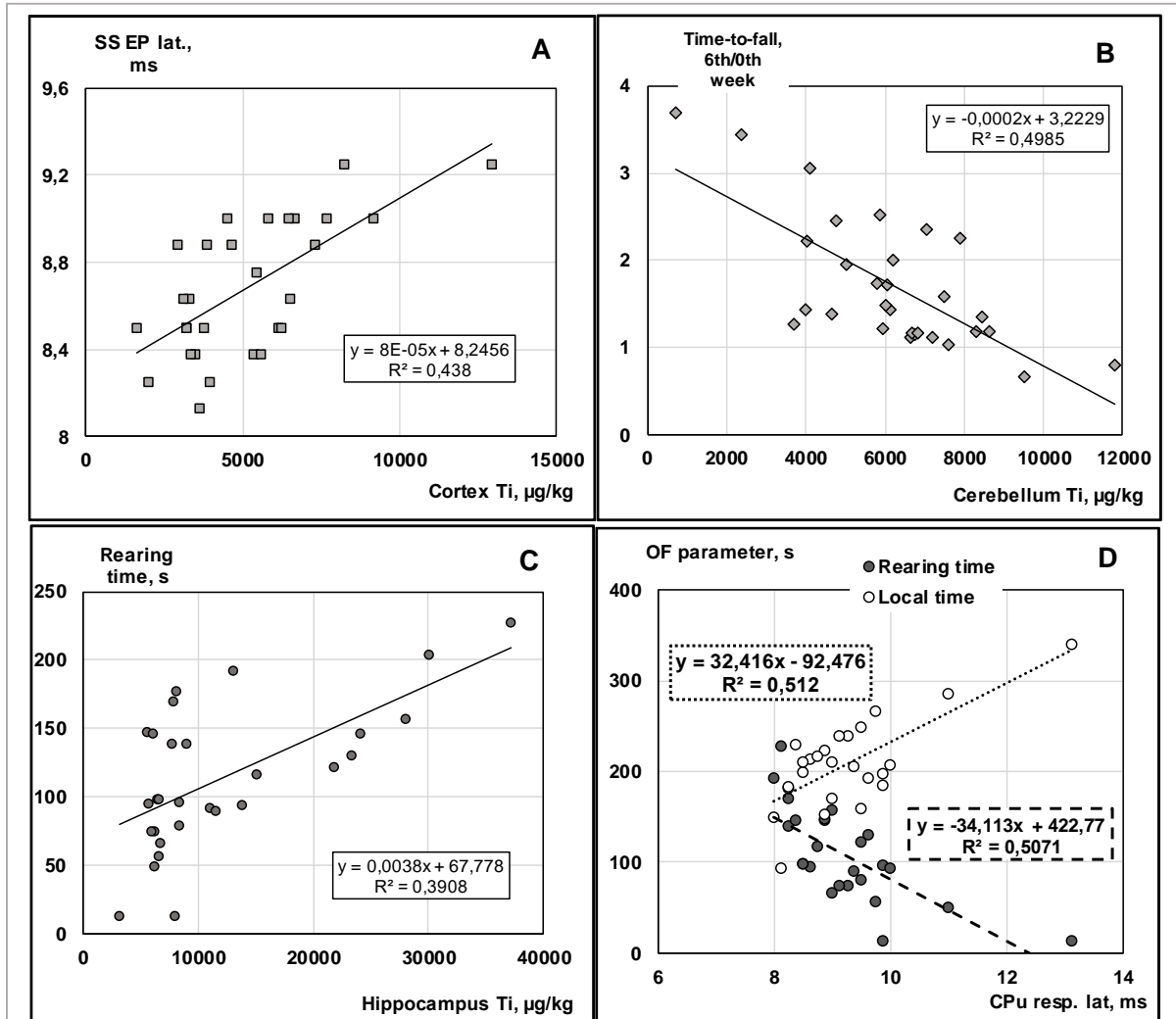


Figure 23: Correlation diagrams of the treated rats' brain Ti levels and the SS EP latency at 10 Hz stimulation (A), climb time ratio on the 6th and 0th week (B) and OF rearing time (C). Correlation diagram of the electrophysiological response from the caudato-putamen and two OF parameters in the treated rats (D). Trend lines fitted and R^2 calculated by Excel.

3.5. Toxic effects of the TiO₂ nanorods on the kidneys

3.5.1. Titanium levels in the kidney samples

The Ti content in the kidneys was significantly elevated in the treated vs. control rats but the increase was not fully proportional to the dose (Table 7). This suggested that the amount of deposition was determined not only by the kidneys' filtration activity but also by the blood Ti level which, at 18 mg/kg b.w. dose, disproportionately increased the amount deposited in the kidneys.

Table 7: Tissue metal levels in the control and treated rats' kidney and blood samples, and image analysis results of the kidney light microscopic sections.

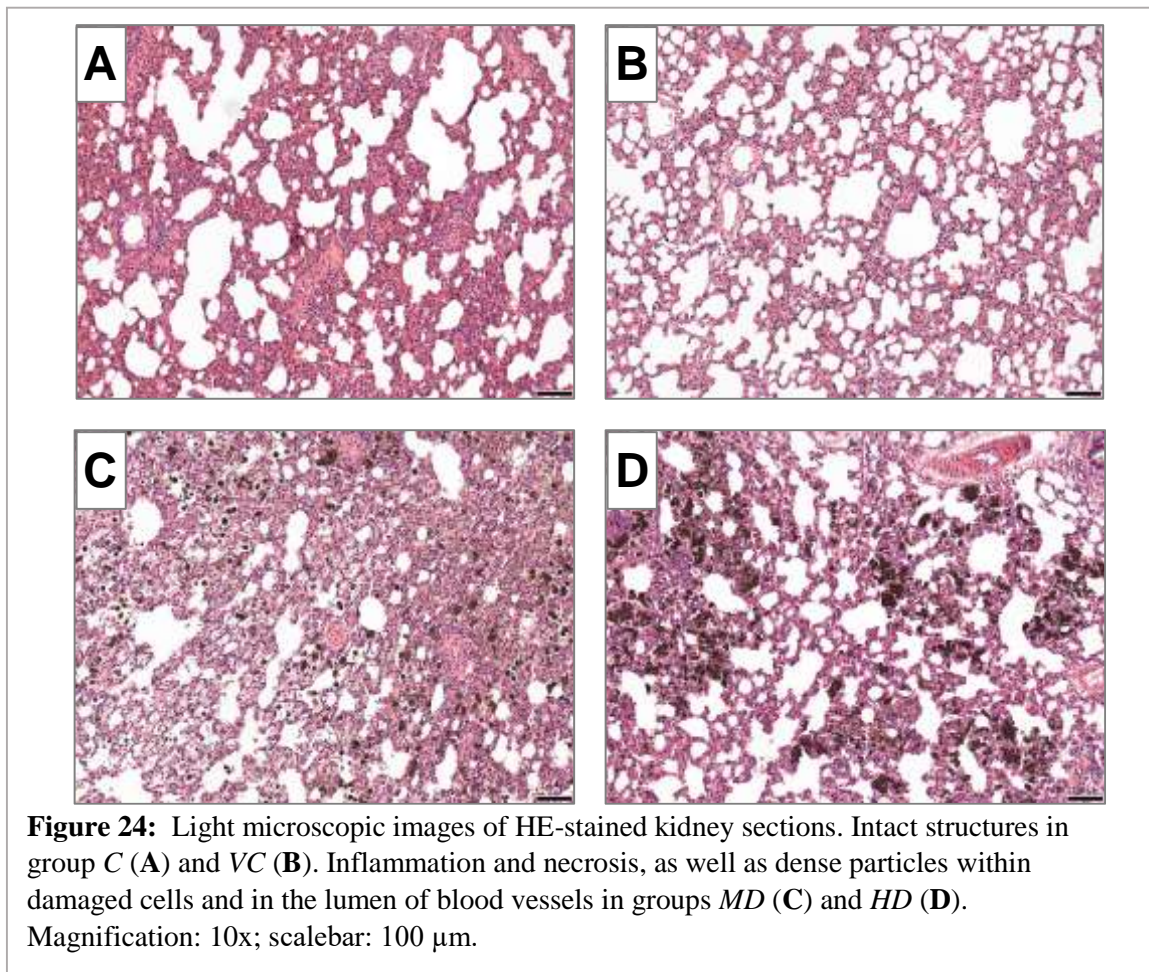
Groups	Tissue Ti levels (mg/kg bw)		ImageJ results (n=10/group)		
	In blood n=8/group	In the kidneys n=10/group	Number of dense grains image	Area	Maximal diameter
<i>C</i>	153.34 ±314.41	1376.21 ± 98.22	-	n.d.	n.d.
<i>VC</i>	205.65 ±387.07	1926.70 ± 560.94	-	n.d.	n.d.
<i>LD</i>	1077.10 ±1672.47	2650.72 ± 1708.64	188	1031.86 ±179.33*** ###	40.77 ±3.88*** ###
<i>MD</i>	1109.23 ±893.51	2979.40 ± 1132.79	223	1080.17 ±327.20***###	41.94 ±6.26***###
<i>HD</i>	1182.69 ± 1887.36	3745.71 ± 612.72**	297	1168.95 ±449.17***###	42.84 ±8.75***###

Mean±SD, n = as indicated.

, *: p<0.01, 0.001 vs. *C*; ###: p<0.001 vs. *VT* (non-parametric ANOVA)

3.5.2. Histopathological findings in the kidneys

The visualized presence of TiO₂ NPs in the kidneys was congruent with the chemically detected Ti. By light microscopy, necrotic glomerular and tubular epithelial cells were seen in the kidney sections of *MD* and *HD* treated rats, together with dark, dense objects – possibly aggregates of NPs phagocytosed by the tubular epithelial cells, similar to those observed in macrophages in the lung sections – which was absent in the sections from groups *C* or *VC* (Fig. 24). By quantitative image analysis, the presence of NP-laden cells appeared to be proportional to both external dose and internal NP load (Table 7).



TEM images (Fig. 25) showed NPs and their aggregates within the cells. In Fig. 25A, proximal tubular epithelium is seen with dark particles in the smooth musculature of the arteriolar wall; in part B, dense grains (apparently NPs) near the brush border, on free cytoplasmic ribosomes and on the rough endoplasmic reticulum. Fig. 25 C and D shows a postglomerular efferent arteriola, with dark grains in the smooth muscular wall attached to free ribosomes, but not in the RBCs. Fig. 25 E and F: preglomerular arteriola with NPs in the cytoplasm of endothelial cell and on the basal membrane. Fig. 25 G and H: proximal tubule, NPs in the cytoplasm of the endothelial cell. Fig. 25 I and J: Henle's loop, accumulated dense grains in the cytoplasm of the endothelial cell and in its nucleus. Occurrence of the NPs in samples from groups *C* and *VC* must have been due to cross-contamination which is also suggested by the measured Ti levels shown in Table 7.

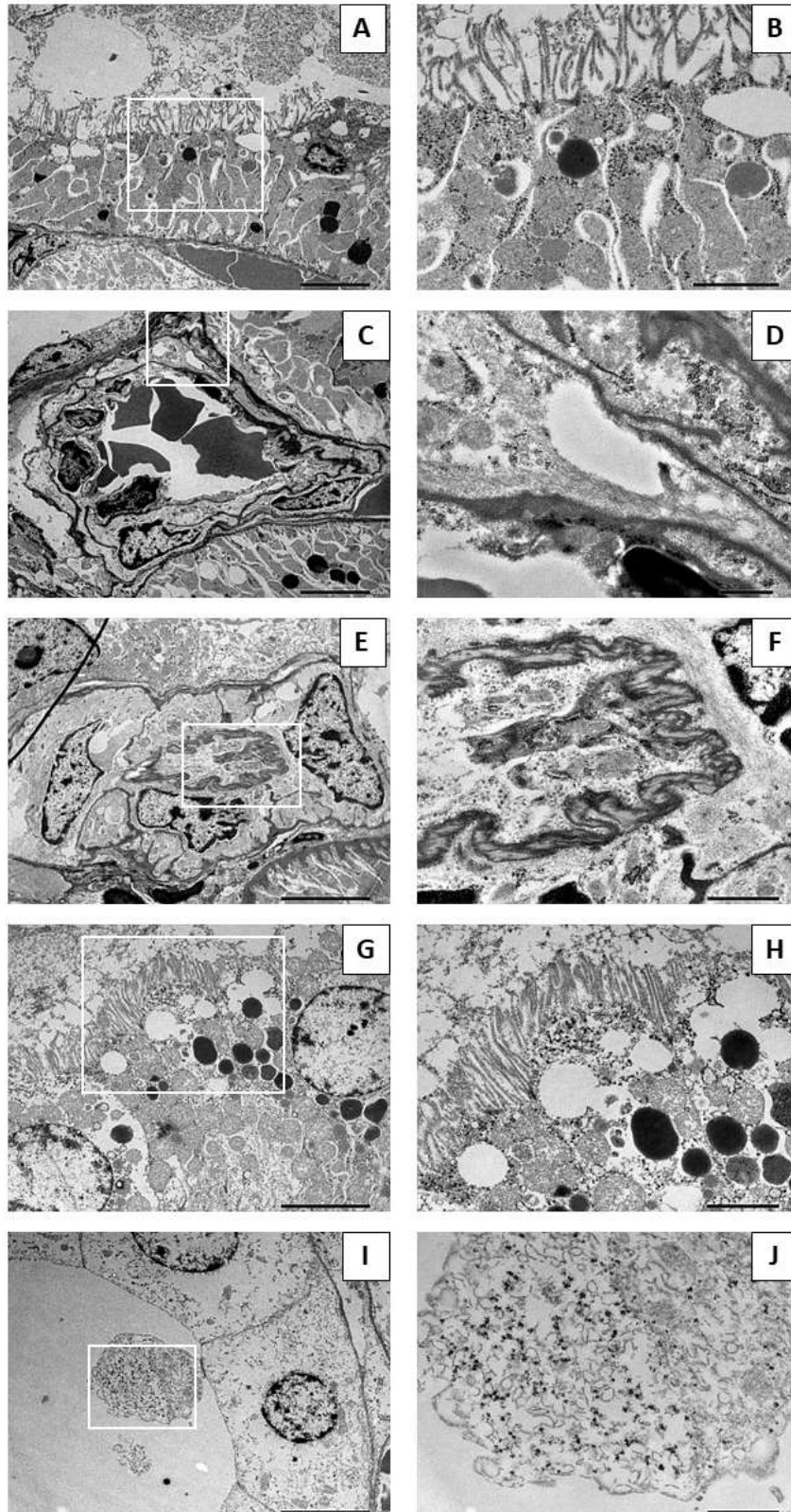


Figure 25: Presence of TiO_2 NPs and aggregates in the rats' kidneys. TEM images from group *C* (**A**, 2000x; **B**, 6000x), *VC* (**C**, 2000x; **D**, 15,000x), *LD* (**E**, 2500x; **F**, 10,000x), *HD*, cortex (**G**, 2500x; **H**, 5000x) and *HD*, medulla (**I**, 2,500x; **J**, 10,000x). White frames in the left row indicate the cutouts shown on the right.

4. DISCUSSION

The experimental results presented above demonstrated that the applicant was successful in eliciting neuro-functional, morphological and biochemical alterations in rats by intratracheal application of TiO₂ nanorods which alterations may have human health relevance. In this aspect, one of the main questions is to what extent the doses used in an animal model correspond to those observed in cases of human exposure.

In case of nano-TiO₂, there are not many data available on occupational exposure. The data by Hext et al. (2005) show that in Europe and North America there were no workplace airborne TiO₂ levels above 1 mg/m³ (for the whole respirable fraction) in the last 20 years. Recommended exposure limits of CDC-NIOSH (2011) are 2.4 mg/m³ for suspended TiO₂ dust and 0.3 mg/m³ for ultrafine dust (that is, for TiO₂ NPs) in a 4 x 10 hours per week exposure scheme. Calculating with the daily ventilation volume of rats (Strohl et al., 1997), the dose of TiO₂ NP applied in the rats' trachea in the present study would approximately mean atmospheric concentrations of 5 to 90 mg/m³. These are about one or two degrees of magnitude higher than the limit recommended by NIOSH, but the length of exposure in the present experiment, 28 days, is a small fraction (ca. 1/30) of the expectable life span of rats and would thus correspond to ca. 2.5 years in humans (a relatively short period in a job career). On the other hand, instilled experimental doses of up to 18 mg/kg are not excessive, as judged on the basis of Shakeel et al. (2016).

However, the real determinant of a toxic effect is internal dose at the site or sites of action. The highest levels of chemically detected Ti and visualized TiO₂ NPs were found in the lungs. This was in partial accordance with Baisch et al. (2014) who reported complete retention of instilled TiO₂ NPs in rat lungs for several days – but we could detect lower amounts of Ti in other organs of interest also, most importantly in the brain and kidneys.

Uptake via the lungs and systemic distribution of TiO₂ (and other) NPs depends, among others, on particle size. Choi et al. (2010) found that, after pulmonary instillation to rats, only NPs below 34 nm size were rapidly transported through the alveolar epithelium to the interstitium and further to local lymph nodes. According to Buckley et al. (2017) iridium NPs of 10 nm showed ca. 5 times more translocation from the lungs to liver and kidneys than 75 nm NPs; underlining the effect of NP size on crossing barriers.

Elevated Ti levels were found in our samples of blood, as well as of organs including brain and kidneys. This fits well with the findings Choi et al. (2010) because (at least in one dimension) the nanorods used by us were in the <34 nm size range.

Translocation of more or less intact NPs by means of phagosomes contained in alveolar macrophages was verified (presence of nanorod-laden macrophages in the hilar lymph nodes: Fig. 8E, 9C-E), and presence of NPs in the kidneys was also shown (Fig. 25). This, together with elevated Ti levels in the treated rats' blood, brain and other tissue samples, outlined the complete fate of TiO₂ NPs and their metal content from uptake through sites of action up to excretion.

For the detected presence of Ti in brain samples, TiO₂ NPs must have crossed the BBB (dissolution of metal ions from their surface in the acidic environment of the phagosomes, as described by Lundborg et al. (1985) is with TiO₂ not likely); but NPs may have migrated to the brain also along afferent nerves – both regarded as feasible (Song et al., 2015). Crossing the BBB was probable because damage to the BBB in rats that inhaled nano-Ti has been observed by Disidier et al. (2017).

Migration of NPs within the (animal or human) organism is typically size-dependent (Choi et al., 2010; Shi et al., 2013). Breakdown of the BBB and neuronal damage caused by ip. administered metal NPs was more severe with 20-30 nm than with 56-60 nm or >100 nm particles (Sharma et al., 2013). In our pre-experiment 2, spherical NPs of ca. 10 nm size had, at equal mg/kg dose, a stronger effect on cortical EPs, and the larger (>100 nm) ones, on grip strength; where the latter effect was probably more dependent on peripheral effects on the motor nerves and muscles involved (see paper No. IV in Appendix).

Once within the brain substance, TiO₂ NPs could cause the observed functional alterations by several mechanisms. First of all, oxidative stress may have played a major role. Nano-TiO₂ used in our experiments had anatase crystal structure which is the chemically more active one (Sayes et al., 2006). To oxidative stress, the nervous system is especially sensitive. Neurons show both intense mitochondrial energy production because of the high energy demand, and abundance of (unsaturated) structural lipids, but their antioxidant defence capacity is low (Guerra-Araiza et al., 2013). ROS have been regarded as “final common pathway” in the action of several neurotoxic agents (LeBel and Bondy, 1991).

Increased lipid peroxidation could be measured in both brain and lung samples of the treated rats. Oxidative damage to membrane lipids is likely to result in changes of membrane fluidity and this way in alterations of membrane-bound events of pulse propagation and synaptic transmission (Coyle and Puttfarcken, 1993). The chain of causal relationships from Ti levels in

organs through oxidative stress up to functional alteration was supported by the correlations observed between electrophysiological and behavioral signs of functional damage, and the level of Ti and TBARS in the brain. In an earlier work of the Department, rats were exposed the same way with another nanoparticulate metal oxide (MnO_2) and the functional alterations (lengthening of EP latency, decreased rearing in the OF) in the treated rats were reversed by antioxidant treatment, supporting the role of oxidative mechanism in NP-induced neuro-functional damage (Sárközi et al., 2013).

In the parameters (latency, amplitude, etc.) of sensory cortical EPs, alterations along the whole sensory pathway – from peripheral endings to cortical neurons – can be represented. Axonal conduction and synaptic transmission, both involved in the generation of EPs, are energy-demanding processes, so that their alteration in states of decreased energy supply is plausible. Mitochondrial damage (together with ROS generation) has been described *in vivo* in human neuronal and glial cell lines on exposure to TiO_2 NPs (Coccini et al., 2015); in which the tendency of NPs to migrate to mitochondria and interfere with oxidative phosphorylation may have played a role (Oberdörster et al., 2005).

In the brain, the resulting energy shortage affects both neuronal and glial cells. Glutamate, the most important central excitatory transmitter, is co-transported into the astrocytes with Na^+ along its concentration gradient. When ion pumps do not operate properly due to energy shortage, failing transport can lead to excess perisynaptic glutamate and disturbed transmission (Takahashi et al., 1997). Weakened ion pumps also impair transmembrane ion gradients required for spike propagation. Similar pattern of changes in EP latency and tail nerve conduction velocity suggested that the effect of TiO_2 NPs on axonal conduction and synaptic transmission were both involved in the mechanism of the observed changes – both at the level of EPs and at behavioral level as in case of lengthened latency of ASR noise positive response. Besides, increased fatigability of the SS sensory pathway (Fig. 19C,D) also suggested energy shortage.

NP-induced oxidative damage to cells in the brain and abnormal transmitter turnover were probably responsible for the behavioral changes observed in the nano- TiO_2 treated rats. Avoidance of the central zone of the OF and of the open arms of the elevated plus maze are accepted indicators of increased anxiety (Griebel and Holmes, 2013). Exploration of a novel place can be regarded as a product of the combined influences of curiosity and fear (Halliday, 1968), and the shift of the exploration–anxiety balance to the latter has been linked to dopaminergic hypofunction both in rats and in humans (Chaudhuri and Schapira 2009; Gass and Wotjak 2013).

Motility depends on mesolimbic and mesocortical dopaminergic neuronal transmission (Fink and Smith, 1980). Dopaminergic neurons are especially sensitive to oxidative stress due to the auto-oxidizing tendency of dopamine and the presence of monoamine oxidase producing hydrogen peroxide (Alexi et al., 2000). This, together with the ROS-generating effect of TiO₂ NPs, may provide the mechanistic basis of the behavioral effects in the OF and EPM tests. In mice, treated intranasally for 30 days with rutile TiO₂ NPs, decreased levels of several monoamines were detected, and the change was parallel with local Ti levels and neuronal damage (Zhang et al., 2011). Also glutamate, beyond its role in the electrophysiological phenomena mentioned above, seems to be included in the mechanism of anxiety (Griebel and Holmes, 2013) and its possibly increased level due to slowed removal from the synapse can be anxiogenic.

One further consequence of oxidative stress caused by TiO₂ NPs is inflammation, developing in case first line antioxidant defence is insufficient (Xiao et al., 2003). In our work, inflammation markers were detected in the exposed rats' lungs. Lysosomes in alveolar macrophages, laden with phagocytosed TiO₂ NPs, probably underwent membrane permeabilization (which may have been aggravated by membrane lipid peroxidation mentioned above). The released lysosomal enzymes, such as cathepsin B, activate caspases (constituents of inflammasomes) that further convert interleukin-1 β to its active form (Boland et al., 2014). Nano-TiO₂ laden phagosomes were seen in also in epithelial cells in kidney sections.

The spectrum of interleukin activation seen in the lung tissue of *HD* rats (Fig. 10) indicated that the inflammation was acute but started to turn to chronic during the treatment period. TiO₂ NPs were described to induce the release of both IL-1 α and IL-1 β (Yazdi et al., 2010). IL-1 α – together with IL-1-ra (interleukin-1 receptor antagonist; another member of the IL-1 group) – was indeed detected in lung tissues of the *HD* group.

CINC-1 (cytokine-induced neutrophil chemoattractant, part of the acute inflammatory reaction: Ghaly and Marsh, 2010) probably induced by the cytokines, is also known to be involved in pulmonary inflammation (Morimoto et al., 2016). The observed inflammogenic effect of the anatase nanorods also explains the presence of the lipopolysaccharide-inducible CXC chemokine (LIX) and the increased production of CCL-5 (chemokine C-C motif ligand 5) in our *HD* rats. Beyond its contributing role to inflammation, IL-1 is also known to promote autophagy (Harris, 2011), the most likely cause of cell death seen in our *in vitro* work (Fig. 13). Infiltration of leukocytes into the pulmonary parenchyma and alveolar space by trans-endothelial migration, as well as increasing interstitial and decreasing alveolar area (Fig. 8C,D) suggested chronic inflammation, requiring coordinated action of several adhesion molecules.

Enhanced presence of L-selectin (a surface molecule on leukocytes required for interaction with the endothelium of blood vessels: Ley, 2003) in the lung tissue of TiO₂ NP exposed animals (Fig. 10) was also in line with that. Increased presence of the pro-angiogenic VEGF, together with L-selectin, indicated that the local inflammation possibly became systemic – raising the possibility of neuroinflammation. Besides that, the treated rats' kidneys also showed massive presence of nano-TiO₂ laden phagosomes in epithelial cells (Fig. 25) so that inflammatory damage to this organ was also likely – all the more that activation of VEGF and L-selectin suggested that inflammation, developing first in the directly affected organ (the lungs), was becoming systemic.

Neuroinflammation appears to be an important aspect of CNS damage resulting from exposure to NPs (Win-Shwe and Fujimaki, 2011). Inhalation of 10 mg/m³ nano-TiO₂ aerosol (daily 6 hours, 5 days a week for 4 weeks) resulted in increased level of inflammation markers and decreased expression of synaptophysin in the brain of rats even without relevant deposition of Ti (Disdier et al., 2017). Synaptophysin is crucially involved in the trafficking of synaptic vesicles (Xie et al., 2017) so its insufficiency is likely to disturb CNS functions. Oral administration of TiO₂ NPs to rats caused decreased brain acetylcholinesterase activity, together with increased IL-6 level and GFAP reactivity, corresponding to neuronal inflammatory damage and reactive gliosis (Grissa et al., 2016). In an *in vivo* study, TiO₂ NPs did no harm to rat dopaminergic neurons cultured alone, but in a primary culture of embryonic rat striatum the neurons underwent apoptosis on the effect of ROS and inflammatory mediators emitted by the microglia activated by phagocytosed TiO₂ NPs. In the same study microglia, cultured alone, were shown to phagocytose the NPs and produce oxidative burst (Long et al., 2007).

According to Gui et al. (2013), IL-6 was also involved in the inflammatory kidney damage on oral TiO₂ NP application in mice, with apoptosis and necrosis leading to loss of glomeruli and tubules, and depositions chemically identified as TiO₂. In rats, Fadda et al. (2018) saw similar kidney tissue damage and increase of inflammatory mediators on high dose oral nano-TiO₂ application. The diffuse glomerular and tubular necrosis observed in our experiment was similar to that described by Zhao et al. (2010). In that work, abdominal injection of anatase NPs evoked histopathological changes and oxidative stress in mice, the latter being partly similar to the effect observed in our treated rats' lungs. Fartkhooni et al. (2016) found hyaline-like deposits, dilated Bowman's capsules, and tissue degeneration suggesting oxidative stress in kidneys of rats after intraperitoneal injection of TiO₂ NPs. By treating rats with TiO₂ nanorods of similar sizes to ours, Meena and Paulraj (2012) observed oxidative stress, swollen glomeruli, and NP-

laden macrophages in the kidneys. All that raises the possibility that in lengthy exposure the excretory capacity of the kidneys, including elimination of TiO₂ NPs, will be impaired.

Conclusion: Nanoparticulate forms of TiO₂, including non-spherical shapes, are used in numerous applications, and can cause human exposure from several, purposeful or accidental, sources. The physicochemical properties of TiO₂ NPs suggest health damaging effects via several possible mechanisms. Experimental results of the PhD work, described and discussed in this thesis, showed that the rod-shaped TiO₂ NPs with anatase crystal structure, when applied to the airways, remained partly in the lungs but partly caused systemic exposure and reached distant organs like the CNS and the kidneys. Damages caused by the NPs were observed in the lungs, kidneys and the nervous system, with oxidative stress as most likely common element. Up to now, such effects were documented in the literature mostly for spherical TiO₂ NPs. The damages observed in our experimental work, especially those in the nervous system, point to the human health relevance of such studies.

Based on the results presented in this thesis, the points of aims listed in 1.3. can be answered as follows:

- By intratracheal instillation of suspended TiO₂ nanorods, effective internal load could be achieved.
- TiO₂ nanorods and/or their metal content were detected in samples of the lungs, CNS, and kidneys – indicating that the NPs crossed biological barriers, and outlining their complete fate from uptake through sites of action up to excretion.
- In the lungs, significant deposition of nano-TiO₂ and signs of oxidative stress were observed. Cytokine activation indicated acute and chronic inflammation.
- It was possible to detect and quantify neuro-functional alterations in the treated rats by the behavioral and electrophysiological methods applied.
- The behavioral alterations in the rats treated with TiO₂ nanorods were mostly related to increased anxiety, suggesting damage to the dopaminergic, and partly glutamatergic, regulation. Changes in the cortical evoked response underlined glutamatergic damage.
- In the treated rats' kidneys, elevated Ti levels were measured. Presence of NPs, and tissue alterations suggesting functional damage were observed.
- In several cases we could demonstrate that the alterations were proportional to the locally determined Ti load.
- Regarding mass production and widespread application of nano-TiO₂, including nanorods, the results presented in this thesis have human health relevance, first of all for those suffering occupational exposure.

5. REFERENCES

1. Abbott Chalew TE, Ajmani GS, Huang H, Schwab KJ. (2013) Evaluating nanoparticle breakthrough during drinking water treatment. *Environ Health Perspect* 121, 1161–1166.
2. Alexi T, Hughes PE, Faull RLM, Williams CE. (1998) 3-nitropropionic acid's lethal triplet: cooperative pathways of neurodegeneration. *Neuroreport* 9, 57–64.
3. Amara S, Khemissi W, Mrad I, Rihane N, Ben Slama I, El Mir L, Jeljeli M, Ben Rhouma K, Abdelmelek H, Sakly M. (2013) Effect of TiO₂ nanoparticles on emotional behavior and biochemical parameters in adult Wistar rats. *Gen Physiol Biophys* 32, 229–234.
4. Antonini JM. (2003) Health effects of welding. *Crit Rev Toxicol* 33, 61–203.
5. Ayres G, Borm P, Cassee FR, Castranova V, Donaldson K, Ghio A, Harrison RM, Hider R, Kelly F, Kooter IM, Marano F, Maynard RL, Mudway I, Nel A, Sioutas C, Smith S, Baeza-Squiban A, Cho A, Duggan S, Froines J. (2008) Evaluating the toxicity of airborne particulate matter and nanoparticles by measuring oxidative stress potential. A Workshop Report and Consensus Statement. *Inhal Toxicol* 20, 75–99.
6. Baisch BL, Corson NM, Wade-Mercer P, Gelein R, Kennell AJ, Oberdörster G, Elder A. (2014) Equivalent titanium dioxide nanoparticle deposition by intratracheal instillation and whole body inhalation: the effect of dose rate on acute respiratory tract inflammation. *Part Fibre Toxicol* 11, 5.
7. Bannerman DM, Rawlins JN, McHugh SB, Deacon RM, Yee BK, Bast T, Zhang WN, Pothuizen HH, Feldon J. (2004) Regional dissociations within the hippocampus—memory and anxiety. *Neurosci Biobehav Rev* 28, 273–283.
8. Beers RF, Sizer IW. (1953) Catalase assay with special reference to manometric methods. *Science* 117, 710–712.
9. Ben-Younes NR, Amara S, Mrad I, Ben-Slama I, Jeljeli M, Omri K, El Ghouli J, El Mir L, Rhouma KB, Abdelmelek H, Sakly M. (2015) Subacute toxicity of titanium dioxide (TiO₂) nanoparticles in male rats: emotional behavior and pathophysiological examination. *Environ Sci Pollut Res* 22, 8728–8737.
10. Berne BJ, Pecora R. (2000) *Dynamic light scattering with applications to chemistry, biology, and physics*. Dover Publications, Mineola, USA.
11. Boffetta P, Gaborieau V, Nadon L, Parent MF, Weiderpass E, Siemiatycki J. (2001) Exposure to titanium dioxide and risk of lung cancer in a population-based study from Montreal. *Scand J Work Environ Health* 27, 227–232.
12. Boland S, Hussain S, Baeza-Squiban A. (2014) Carbon black and titanium dioxide nanoparticles induce distinct molecular mechanisms of toxicity. *Rev Nanomed Nanobiotechnol* 6, 641–652.
13. Bradford MM. (1976) A rapid and sensitive method for the quantitation of microgram quantities of protein utilizing the principle of protein-dye binding. *Anal Biochem* 72, 248–254.
14. Buckley A, Warren J, Hodgson A, Marczylo T, Ignatyev K, Guo C. (2017) Slow lung clearance and limited translocation of four sizes of inhaled iridium nanoparticles. *Part Fibre Toxicol* 14, 5.
15. Buzea C, Pacheco Blandino II, Robbie K. (2007) Nanomaterials and nanoparticles: Sources and toxicity. *Biointerphases* 2, MR17–MR172.
16. Carobrez AP, Bertoglio LJ. (2005) Ethological and temporal analyses of anxiety-like behavior: The elevated plus-maze model 20 years on. *Neurosci Biobehav Rev* 29, 1193–1205.
17. CDC-NIOSH (2011): *Occupational Exposure to Titanium Dioxide*. Current Intelligence Bulletin 63. Centers for Disease Control and Prevention, National Institute for Occupational Safety and Health, USA.
18. Chaudhuri KR, Schapira AHV. (2009) Non-motor symptoms of Parkinson's disease: dopaminergic pathophysiology and treatment. *Lancet Neurol* 8, 464–474.
19. Chen J, Poon C. (2009) Photocatalytic construction and building materials: From fundamentals to applications. *Building Environ* 44, 1899–1906.
20. Choi HS, Ashitate Y, Lee JH, Kim SH, Matsui A, Insin N, Bawendi MG, Semmler-Behnke M, Frangioni JV, Tsuda A. (2010) Rapid translocation of nanoparticles from the lung airspaces to the body. *Nat Biotechnol* 28, 1300–1303.
21. Coccini T, Grandi S, Lonati D, Locatelli C, De Simone U. (2015) Comparative cellular toxicity of titanium dioxide nanoparticles on human astrocyte and neuronal cells after acute and prolonged exposure. *Neurotoxicol* 48, 77–89.

22. Coyle JT, Puttfarcken P (1992): Oxidative stress, glutamate and neurodegenerative disorders. *Science* 262, 689–695.
23. Czajka M, Sawicki K, Sikorska K, Poppek S, Kruszewski M, Kapka-Skrzypczak L. (2015) Toxicity of titanium dioxide nanoparticles in central nervous system. *Toxicol In Vitro* 29, 1042–1052.
24. Dalle-Donne I, Rossi R, Giustarini D. (2003) Protein carbonyl groups as biomarkers of oxidative stress. *Clin Chim Acta* 329, 23–38.
25. Dastjerdi R, Montazer M. (2010) A review on the application of inorganic nano-structured materials in the modification of textiles: Focus on anti-microbial properties. *Colloids Surf B Biointerfaces* 79, 5–18.
26. Debia M, Bakhiyi B, Ostiguy C, Verbeek JH, Brouwer DH, Murashov V. (2016) A Systematic Review of Reported Exposure to Engineered Nanomaterials. *Ann Occup Hyg* 60, 916–935.
27. Decree No. 14/2001 (V. 9.) KöM-EüM-FVM együttes rendelet a légszennyezettségi határértékekről, a helyhez kötött légszennyező pontforrások kibocsátási határértékeiről. *Magyar Közlöny* 2001/53, 3512–3538.
28. Disdier C, Chalansonnet M, Gagnaire F, Gaté L, Cosnier F, Devoy J, Saba W, Lund AK, Brun E, Mabondzo A. (2017) Brain inflammation, blood brain barrier dysfunction and neuronal synaptophysin decrease after inhalation exposure to titanium dioxide nano-aerosol in aging rats. *Scientific Reports* 7, 12196.
29. Dockery DW, Pope CA III, Xu X, Spengler J, Ware JH, Fay ME, Ferris BG, Speizer FE. (1993) An association between air pollution and mortality in six US cities. *NEJM* 329, 1753–1759.
30. Donaldson K, Tran CL. (2002) Inflammation caused by particles and fibers. *Inhal Toxicol* 14, 5–27.
31. Dunham NW, Miya TS. (1957) A note on a simple apparatus for detecting neurological deficit in rats and mice. *J Am Pharm Assoc* 46, 208–209.
32. EFSA ANS Panel (EFSA Panel on Food Additives and Nutrient Sources added to Food). (2016) Scientific Opinion on the re-evaluation of titanium dioxide (E 171) as a food additive. *EFSA Journal* 14, 45–45.
33. Elsaesser A, Howard CV. (2012) Toxicology of nanoparticles. *Adv Drug Deliv Rev* 64, 129–137.
34. Erriquez J, Bolis V, Morel S, Fenoglio I, Fubini B, Quagliotto P, Distasi C. (2015) Nanosized TiO₂ is internalized by dorsal root ganglion cells and causes damage via apoptosis. *Nanomedicine* 11, 1309–1319.
35. European Agency for Safety and Health at Work. (2009) Expert forecast on emerging chemical risks related to occupational safety and health. ISBN 978-92-9191-171-4.
36. European Council (2008). Directive 2008/1/EC of the European Parliament and the Council of 15 January 2008 concerning integrated pollution prevention and control. *Official Journal L24*, 8–29.
37. Fadda LM, Mohamed AM, Ali HM, Hagar H, Aldossari M. (2018) Prophylactic administration of carnosine and melatonin abates the incidence of renal toxicity induced by an over dose of titanium dioxide nanoparticles. *J Biochem Mol Toxicol* 32, e22040.
38. Fartkhooni FM, Noori A, Mohammadi A. (2016) Effects of titanium dioxide nanoparticles. Toxicity on the kidney of male rats. *Int J Life Sci* 10, 65–69.
39. Feng Q, Ma Y, Mu S, Wu J, Chen S, Ou-Yang L, Lei W. (2014) Specific reactions of different striatal neuron types in morphology induced by quinolinic acid in rats. *PLoS ONE* 9, e91512.
40. Fink JS, Smith GP. (1980) Mesolimbic and neocortical dopaminergic neurons are necessary for normal exploratory behavior in rats. *Neurosci Lett* 17, 61–65.
41. Gao X, Yin S, Tang M, Chen J, Yang Z, Zhang W, Chen L, Yang B, Li Z, Zha Y, Ruan D, Wang M. (2011) Effects of developmental exposure to TiO₂ nanoparticles on synaptic plasticity in hippocampal dentate gyrus area: an in vivo study in anesthetized rats. *Biol Trace Elem Res* 143, 1616–1628.
42. Garabant DH, Fine LJ, Oliver C, Bernstein L, Peters JM. (1987) Abnormalities of pulmonary function and pleural disease among titanium metal production workers. *Scand J Work Environ Health* 13, 47–51.
43. Gass P, Wotjak C. (2013) Rodent models of psychiatric disorders – practical considerations. *Cell Tissue Res* 354, 1–7.
44. Ghaly A, Marsh DR. (2010) Ischaemia-reperfusion modulates inflammation and fibrosis of skeletal muscle after contusion injury. *Int J Exp Pathol* 91, 244–255.

45. Gifkins A, Greba Q, Kokkimidis L. (2002) Ventral tegmental area DA neurons mediate the shock sensitisation of acoustic startle: A potential site of action for benzodiazepine anxiolytics. *Behav Neurosci* 116, 785–794.
46. Giovanni M, Tay CH, Setyawati MI, Xie J, Ong CN, Fan R, Yue J, Zhang L, Leong DT. (2015) Toxicity Profiling of Water Contextual Zinc Oxide, Silver, and Titanium Dioxide Nanoparticles in Human Oral and Gastrointestinal Cell Systems. *Environ Toxicol* 30, 1459–1469.
47. Gondikas AP, von der Kammer F, Reed RB, Wagner S, Ranville JF, Hofmann T. (2014) Release of TiO₂ Nanoparticles from Sunscreens into Surface Waters: A One-Year Survey at the Old Danube Recreational Lake. *Environ Sci Technol* 48, 5415–5422.
48. González-Esquivel AE, Charles-Niño CL, Pacheco-Moisés FP, Ortiz GG, Jaramillo-Juárez, Rincón-Sánchez AR. (2015) Beneficial effects of quercetin on oxidative stress in liver and kidney induced by titanium dioxide (TiO₂) nanoparticles in rats. *Toxicol Mech Meth* 25, 166–175.
49. Gramowski A, Flossdorf J, Bhattacharya K, Jonas L, Lantow M, Rahman Q, Schiffmann D, Weiss DG, Dopp E. (2010). Nanoparticles induce changes of the electrical activity of neuronal networks on microelectrode array neurochips. *Environ Health Perspect* 118, 1363–1369
50. Grande F, Tucci P. (2016) Titanium dioxide nanoparticles: a risk for human health? *Mini Rev Med Chem* 16, 762–769.
51. Griebel G, Holmes A. (2013) 50 years of hurdles and hope in anxiolytic drugdiscovery. *Nat Rev Drug Discov* 12, 667–687.
52. Grissa I, Guezguez S, Ezzi L, Chakroun S, Sallem A, Kerkeni E, Elghoul J, El Mir L, Mehdi M, Cheikh HB, Haouas Z. (2016) The effect of titanium dioxide nanoparticles on neuroinflammation response in rat brain. *Environ Sci Pollut Res Int* 20, 20205–20213.
53. Groh KS, Geueke B, Muncke J. (2017) Food contact materials and gut health: Implications for toxicity assessment and relevance of high molecular weight migrants. *Food Chem Toxicol* 109, 1–18.
54. Guerra-Araiza C, Álvarez-Mejía AL, Sánchez-Torres S, Farfan-García E, Mondragón-Lozano R, Pinto-Almazán R, Salgado-Ceballos H. (2013) Effect of natural exogenous antioxidants on aging and on neurodegenerative diseases. *Free Rad Res* 47, 451–462.
55. Gui S, Sang X, Zheng L, Ze Y, Zhao X, Sheng L, Sun Q, Cheng Z, Cheng J, Hu R, Wang L, Hong F, Tang M. (2013) Intragastric exposure to titanium dioxide nanoparticles induced nephrotoxicity in mice, assessed by physiological and gene expression modifications. *Part Fibre Toxicol* 10, 4.
56. Halliday MS. (1968) Exploratory behavior. In: Weiskrantz L, editor. *Analysis of behavioral change*. New York: Harper and Row.
57. Harris J. (2011) Autophagy and cytokines. *Cytokine* 56, 140–144.
58. Hext PM, Tomenson JA, Thompson P. (2005) Titanium dioxide: Inhalation toxicology and epidemiology. *Ann Occup Hyg* 49, 461–472.
59. Hu R, Gong X, Duan Y, Li N, Che Y, Cui Y, Zhou M, Liu C, Wang H, Hong F. (2010) Neurotoxicological effects and the impairment of spatial recognition memory in mice caused by exposure to TiO₂ nanoparticles. *Biomaterials* 31, 8043–8050.
60. Huerta-García E, Márquez-Ramírez SG, Ramos-Godinez M, López-Saavedra A, Herrera LA, Parra A, Alfaro-Moreno E, Gomez EO, López-Marure R. (2015) Internalization of titanium dioxide nanoparticles by glial cells is given at short times and is mainly mediated by actin reorganization-dependent endocytosis. *Neurotoxicol* 51, 27–37.
61. IARC Working Group on the Evaluation of Carcinogenic Risks to Humans. (2006) Carbon black, titanium dioxide, and talc. IARC monographs on the evaluation of carcinogenic risks to humans 93, 193–275.
62. ICDD (2018) International Centre for Diffraction Data, PDF-4/Minerals 2018. Newton Square, PA, USA. Available from: www.icdd.com/index.php/pdf-4minerals. Accessed 7 May 2018.
63. ICRP (International Commission on Radiation Protection) (1994). Human respiratory tract model for radiological protection. A report of a task group of the ICRP. *Ann Int Comm Rad Protect* 24, 1–300.
64. Kahru A, Dubourguier HC. (2010) From ecotoxicology to nanoecotoxicology. *Toxicology* 269, 105–119.
65. Kandel ER, Schwartz JH. (1985) *Principles of Neural Science*. Elsevier, New York, pp. 643–644.
66. Kobayashi N, Naya M, Endoh S, Maru J, Yamamoto K, Nakanishi J. (2009) Comparative pulmonary toxicity study of nano-TiO₂ particles of different sizes and agglomerations in rats: Different short- and long-term post-instillation results. *Toxicology* 264, 110–118.

67. Koblin DD. (2002) Urethane: Help or hindrance? *Anesth Analg* 94, 241–242.
68. Koch M, Schnitzler HU. (1997) The acoustic startle response in rats – circuits mediating evocation, inhibition and potentiation. *Behav Brain Res* 89, 35–49.
69. Koch M. (1999) The neurobiology of startle. *Prog Neurobiol* 59, 107–128.
70. Koivisto AJ, Lyyräinen J, Auvinen A, Vanhala E, Hämeri K, Tuomi T, Jokiniemi J. (2012) Industrial worker exposure to airborne particles during the packing of pigment and nanoscale titanium dioxide. *Inhal Toxicol* 24, 839–849.
71. Kreyling WG, Semmler-Behnke M, Moeller W. (2006) Health implications of nanoparticles. *J Nanopart Res* 8, 543–562.
72. Kwon S, Yang YS, Yang HS, Lee J, Kang MS, Lee BS, Lee K, Song CW. (2012) Nasal and pulmonary toxicity of titanium dioxide nanoparticles in rats. *Toxicol Res* 28, 217–224.
73. Laden F, Schwartz J, Speizer FE, Dockery DW. (2006) Reduction in fine particulate air pollution and mortality. Extended follow-up of the Harvard six cities study. *Am J Respir Crit Care Med* 173, 667–672.
74. Le BC, Bondy SC. (1991) Oxygen radicals: common mediators of neurotoxicity. *Neurotoxicol Teratol* 13, 341–346.
75. Ley K. (2003) The role of selectins in inflammation and disease. *Trends Mol Med* 9, 263–268.
76. Li M, Yin JJ, Wamer WG, Lo YM. (2014) Mechanistic characterization of titanium dioxide nanoparticle-induced toxicity using electron spin resonance. *J Food Drug Anal* 22, 76–85.
77. Lieber M, Smith B, Szakal A, Nelson-Rees W, Todaro G. (1976) A continuous tumor-cell line from a human lung carcinoma with properties of type II alveolar epithelial cells. *Int J Cancer* 17, 62–70.
78. Ling MP, Chio CP, Chou WC, Chen WY, Hsieh NH, Lin YJ, Liao CM. (2011) Assessing the potential exposure risk and control for airborne titanium dioxide and carbon black nanoparticles in the workplace. *Environ Sci Pollut Res* 18, 877–889.
79. Liu Y, Xu Z, Li X. (2013) Cytotoxicity of titanium dioxide nanoparticles in rat neuroglia cells, *Brain Injury* 27, 934–939.
80. Long TC, Tajuba J, Sama P, Saleh N, Swartz C, Parker J, Hester S, Lowry GV, Veronesi B. (2007) Nanosize titanium dioxide stimulates reactive oxygen species in brain microglia and damages neurons in vitro. *Environ Health Perspect* 115, 1631–1637.
81. Lundborg M, Eklund A, Lind DB, Camner P. (1985) Dissolution of metals by human and rabbit alveolar macrophages. *Brit J Ind Med* 42, 642–645.
82. Meena R, Paulraj R. (2012) Oxidative stress mediated cytotoxicity of TiO₂ nano anatase in liver and kidney of Wistar rat. *Toxicol Env Chem* 94, 146–163.
83. Morimoto Y, Izumi H, Yoshiura Y, Tomonaga T, Lee BW, Okada T, Oyabu T, Myojo T, Kawai K, Yatera K, Shimada M, Kubo M, Yamamoto K, Kitajima S, Kuroda E, Horie M, Kawaguchi K, Sasaki T. (2016) Comparison of pulmonary inflammatory responses following intratracheal instillation and inhalation of nanoparticles. *Nanotoxicology* 10, 607–618.
84. Nel A, Yia T, Mädler L, Li N. (2006) Toxic potential of materials at the nanolevel. *Science* 311, 622–627.
85. Noël A, Charbonneau M, Cloutier Y, Tardif R, Truchon G. (2013) Rat pulmonary responses to inhaled nano-TiO₂: effect of primary particle size and agglomeration state. *Part Fibre Toxicol* 10, 48.
86. Nohynek GJ, Dufour EK. (2012) Nano-sized cosmetic formulations or solid nanoparticles in sunscreens: a risk to human health? *Arch Toxicol* 8, 1063–1075.
87. Oberdörster G, Oberdörster E, Oberdörster J. (2005) Nanotoxicology: An emerging discipline evolving from studies of ultrafine particles. *Environ Health Perspect* 113, 823–839.
88. Oberdörster G. (2000) Toxicology of ultrafine particles: in vivo studies. *Phil Trans R Soc Lond A* 358, 2719–2740.
89. OECD. (2004) Guidance Document for Neurotoxicity Testing. ENV/JM/MONO(2004)25, OECD Environment Directorate, Environment, Health and Safety Division, Paris.
90. Oleru UG. (1987) Respiratory and nonrespiratory morbidity in a titanium oxide paint factory in Nigeria. *Am J Ind Med* 12, 173–180.
91. Oszlanczi G, Horváth E, Szabó A, Horváth E, Sági A, Kozma G, Kónya Z, Paulik E, Nagymajtényi L, Papp A. (2015) Subacute exposure of rats by metal oxide nanoparticles through the airways: general toxicity and neuro-functional effects. *Acta Biol Szeged* 54, 165–170.

92. Oszlánczi G, Vezér T, Sárközi L, Horváth E, Kónya Z, Papp A. (2010) Functional neurotoxicity of Mn-containing nanoparticles in rats. *Ecotox Environ Saf* 73, 2004–2009.
93. Papp A, Pecze L, Vezér T. (2004) Dynamics of central and peripheral evoked electrical activity in the nervous system of rats exposed to xenobiotics. *Centr Eur J Occup Environ Med* 10, 52–59.
94. Paxinos G, Watson C. (1982) *The rat brain in stereotaxic coordinates*. Academic Press, New York.
95. Pelclova D, Zdimal V, Fenclova Z, Vlckova S, Turci F, Corazzari I, Kacer P, Schwarz J, Zikova N, Makes O, Syslova K, Komarc M, Belacek J, Navratil T, Machajova M, Zakharov S. (2016) Markers of oxidative damage of nucleic acids and proteins among workers exposed to TiO₂ (nano) particles. *Occup Environ Med* 73, 110–118.
96. Pröfrock D, Prange A. (2012) Inductively coupled plasma-mass spectrometry (ICP-MS) for quantitative analysis in environmental and life sciences: a review of challenges, solutions, and trends. *Appl Spectrosc* 66, 843–868.
97. Pryor GT, Ueno ET, Tilson HA, Mitchell LC. (1983) Assessment of chemicals using a battery of neurobehavioral tests: a comparative study. *Neurobehav Toxicol Teratol* 5, 91–117.
98. Pujalté I, Dieme D, Haddad S, Serventi AM, Bouchard M. (2017) Toxicokinetics of titanium dioxide (TiO₂) nanoparticles after inhalation in rats. *Toxicol Lett* 265, 77–85.
99. Ramanakumar AV, Parent ME, Latreille B, Siemiatycki J. (2008) Risk of lung cancer following exposure to carbon black, titanium dioxide and talc: Results from two case-control studies in Montreal. *Int J Cancer* 122, 183–189.
100. Ramirez-Moreno DF, Sejnowski TJ. (2012) A computational model for the modulation for the modulation of the prepulse inhibition of the acoustic startle reflex. *Biol Cybern* 106, 169–176.
101. Ravenzwaay van B, Landsiedel R, Fabian E, Burkhardt S, Strauss V, Ma-Hock L. (2009) Comparing fate and effects of three particles of different surface properties: Nano-TiO₂, pigmentary TiO₂ and quartz. *Toxicol Lett* 186, 152–159.
102. Razani B, Lisanti MP. (2001) Caveolins and caveolae: molecular and functional relationships. *Exp Cell Res* 271, 36–44.
103. Rieger AM, Nelson KL, Konowalchuk JD, Barreda DR. (2011) Modified Annexin V/propidium iodide apoptosis assay for accurate assessment of cell death. *J Vis Exp* 50, e2597.
104. Sager TM, Kommineni C, Castranova V. (2008) Pulmonary response to intratracheal instillation of ultrafine versus fine titanium dioxide: role of particle surface area. *Part Fibre Toxicol* 5, 17.
105. Sárközi K, Nagy V, Papp A, Tombácz E, Szabó A. (2013) The effect of three natural antioxidants on the general and nervous system toxicity of manganese nanoparticles in rats. *Centr Eur J Occup Environ Health* 19, 31–42.
106. Sayes CM, Wahi R, Kurian PA, Liu Y, West JL, Ausman KD, Warheit DB, Colvin VL. (2006) Correlating Nanoscale Titania Structure with Toxicity: A Cytotoxicity and Inflammatory Response Study with Human Dermal Fibroblasts and Human Lung Epithelial Cells. *Toxicol Sci* 92, 174–185.
107. SCENIHR -Scientific Committee on Emerging and Newly Identified Health Risks. (2009) Risk assessment of products of nanotechnologies http://ec.europa.eu/health/ph_risk/committees/04_scenihhr/docs/scenihhr_o_023.pdf
108. Schneider CA, Rasband WS, Eliceiri KW. (2012) NIH Image to ImageJ: 25 years of image analysis. *Nature Meth* 9, 671–675.
109. Serbinova E, Khwaja S, Reznick AZ, Packer L. (1992) Thioctic acid protects against ischemia-reperfusion injury in the isolated perfused Langendorff heart. *Free Rad Res Comm* 17, 49–58.
110. Shakeel M, Jabeen F, Shabbir S, Asghar MS, Khan MS, Chaudhry AS. (2016) Toxicity of nano-titanium dioxide (TiO₂-NP) through various routes of exposure: a review. *Biol Trace Elem Res* 172, 1–36.
111. Sharma A, Muresanu DF, Patnaik R, Sharma HS. (2013) Size- and age-dependent neurotoxicity of engineered metal nanoparticles in rats. *Mol Neurobiol* 8, 386–396.
112. Shi H, Magaye R, Castranova V, Zhao J. (2013) Titanium dioxide nanoparticles: a review of current toxicological data. *Part Fibre Toxicol* 10, 15.
113. Song B, Liu J, Feng X, Wei L, Shao L. (2015) A review on potential neurotoxicity of titanium dioxide nanoparticles. *Nanoscale Res Lett* 10, 342.
114. Stern ST, Adisheshaiah PP, Crist RM. (2012) Autophagy and lysosomal dysfunction as emerging mechanisms of nanomaterial toxicity. *Part Fibre Toxicol* 9, 20.

115. Strohl KP, Thomas AJ, St. Jean P, Schlanker EH, Koletsky RJ, Schork NJ. (1997) Ventilation and metabolism among rat strains. *J Appl Physiol* 82, 317–323.
116. Suh WH, Suslick KS, Stucky GD, Suh YH. (2009) Nanotechnology, nanotoxicology, and neuroscience. *Prog Neurobiol* 87, 133–170.
117. Takahashi M, Billups B, Rossi D, Sarantis M, Hamann M, Attwell D. (1997) The role of glutamate transporters in glutamate homeostasis in the brain. *J Exp Biol* 200, 401–409.
118. Tan MH, Commens CA, Burnett L, Snitch PJ. (1996) A pilot study on the percutaneous absorption of microfine titanium dioxide from sunscreens. *Australas J Dermatol* 37, 185–187.
119. Thurn KT, Arora H, Paunesku T, Wu A, Brown EMB, Doty C, Kremer J, Woloschak G. (2011) Endocytosis of titanium dioxide nanoparticles in prostate cancer PC-3M cells. *Nanomedicine* 7, 123–130.
120. Topuzogullari M, Koc RC, Isoglu SD, Bagirova M, Akdeste Z, Elcicek S, Oztel ON, Baydar SY, Ates SC, Allahverdiyev AM. (2013) Conjugation, characterization and toxicity of lipophosphoglycanpolyacrylic acid conjugate for vaccination against leishmaniasis. *J Biomed Sci* 20, 35.
121. Ursini CL, Cavallo D, Fresegna AM, Ciervo A, Maiello R, Tassone P, Buresti G, Casciardi S, Iavicoli S. (2014) Evaluation of cytotoxic, genotoxic and inflammatory response in human alveolar and bronchial epithelial cells exposed to titanium dioxide nanoparticles. *J Appl Toxicol* 34, 1209–1219.
122. US Environmental Protection Agency. (2003) Impacts of manufactured nanomaterials on human health and the environment. http://www.epa.gov/ncer/rfa/current/2003_nano.html Accessed 26 June 2015.
123. Valdíglesias V, Costa C, Sharma V, Kiliç G, Pásaro E, Teixeira JP, Dhawan A, Laffon B. (2013) Comparative study on effects of two different types of titanium dioxide nanoparticles on human neuronal cells. *Food Chem Toxicol* 57, 352–361.
124. Valko M, Morris H, Cronin MTD. (2005) Metals, toxicity and oxidative stress. *Curr Med Chem* 12, 1161–1208.
125. Walf AA, Frye CA. (2007) The use of the elevated plus maze as an assay of anxiety-related behaviour in rodents. *Nat Protoc* 2, 322–328.
126. Warheit DB, Donner EM. (2015) Risk assessment strategies for nanoscale and fine-sized titanium dioxide particles: Recognizing hazard and exposure issues. *Food Chem Toxicol* 85, 138–147.
127. Weir A, Westerhoff P, Fabricius L, von Goetz N. (2012) Titanium Dioxide Nanoparticles in Food and Personal Care Products. *Environ Sci Technol* 46, 2242–2250.
128. Wiesenthal A, Hunter L, Wang S, Wickliffe J, Wilkerson M. (2011) Nanoparticles: small and mighty. *Int J Dermatol* 50, 247–254.
129. Win-Shwe TT, Fujimaki H. (2011) Nanoparticles and Neurotoxicity. *Int J Mol Sci* 12, 6267–6280.
130. Wu JH, Liu W, Xue CB, Zhou SC, Lan FL, Bi L, Xu HB, Yang XL, Zeng FD. (2009) Toxicity and penetration of TiO₂ nanoparticles in hairless mice and porcine skin after subchronic dermal exposure. *Toxicol Lett* 191, 1–8.
131. Xiao GG, Wang M, Li N, Loo JA, Nel AE. (2003) Use of proteomics to demonstrate a hierarchical oxidative stress response to diesel exhaust particle chemicals in a macrophage cell line. *J Biol Chem* 278, 50781–50790.
132. Xie Z, Long J, Liu J, Chai Z, Kang X, Wang C. (2017) Molecular Mechanisms for the Coupling of Endocytosis to Exocytosis in Neurons. *Frontiers Mol Sci* 10, 47.
133. Yazdi AS, Guarda G, Riteau N, Drexler SK, Tardivel A, Couillin I, Tschopp J. (2010) Nanoparticles activate the NLR pyrin domain containing 3 (Nlrp3) inflammasome and cause pulmonary inflammation through release of IL-1 α and IL-1 β . *PNAS* 107, 19449–19454.
134. Yeomans JS, Frankland PW. (1995) The acoustic startle reflex: neurons and connections. *Brain Res Rev* 21, 301–314.
135. Yoshiura Y, Izumi H, Oyabu T, Hashiba M, Kambara T, Mizuguchi Y, Lee BW, Okada T, Tomonaga T, Myojo T, Yamamoto K, Kitajima S, Horie M, Kuroda E, Morimoto Y. (2015) Pulmonary toxicity of well-dispersed titanium dioxide nanoparticles following intratracheal instillation. *J Nanopart Res* 17, 241.
136. Zandieh S, Hopf R, Redl H, Schlag MG. (2003) The effect of ketamine/xylazine anesthesia on sensory and motor evoked potentials in the rat. *Spinal Cord* 41, 16–22.
137. Ze Y, Sheng L, Zhao X, Ze X, Wang X, Zhou Q, Liu J, Yuan Y, Gui S, Sang X, Sun Q, Hong J, Yu X, Wang L, Li B, Hong F. (2014) Neurotoxic characteristics of spatial recognition damage of the hippocampus in mice following subchronic peroral exposure to TiO₂ nanoparticles. *J Hazard Mat* 264, 219–229.

138. Zhang L, Bai R, Li B, Ge C, Du J, Liu Y, Le Guyader L, Zhao Y, Wu Y, He S, Ma Y, Chen, C. (2011) Rutile TiO₂ particles exert size and surface coating dependent retention and lesions on the murine brain. *Toxicology Letters* 207, 73–81.
139. Zhao J, Li N, Wang S, Zhao X, Wang J, Yan J, Ruan J, Wang H, Hong F. (2010) The mechanism of oxidative damage in the nephrotoxicity of mice caused by nano-anatase TiO₂. *J Exp Nanosci* 5, 447–462.
140. Zhao L, Zhu Y, Chen Z, Xu H, Zhou J, Tang S, Xu Z, Kong F, Li X, Zhang Y, Li X, Zhang J, Jia G. (2018) Cardiopulmonary effects induced by occupational exposure to titanium dioxide nanoparticles. *Nanotoxicology* 12, 169–184.
141. Zilles K. (1984) *The cortex of the rat. A stereotaxic atlas.* Springer, Berlin.

6. ACKNOWLEDGEMENT

I would like to thank to Dr. Edit Paulik, Head of Department of Public Health, because she managed to secure the background, especially finances, to my work.

I am mostly grateful to my supervisors, Dr. Tünde Vezér and Dr. András Papp, who guided me throughout my studies and experimental work. I could always turn to them, and their helpful advice was crucial in the thesis coming to existence.

I thank to the members of the experimental group – Dr. Edina Horváth, Dr. Anita Lukács, Dr. Zsuzsanna Máté, Dr. Andrea Szabó, Dr. Gábor Oszlanczi – for their precious contribution and support in carrying out and evaluating the experiments.

Special thanks to my colleagues who kept my soul in and encouraged me - Dr. Emese Petra Balogh, Dr. Dóra Júlia Eszes, Dr. Mária Markó-Kucsera.

This PhD work would not have been possible without the valuable cooperation of other departments of the university. So I am thankful to:

Dr. Zoltán Kónya and Dr. Gábor Kozma at the Department of Applied and Environmental Chemistry, Faculty of Science and Informatics, for financing, manufacturing and characterizing the various nanoparticles used in the experiments;

Dr. Mónika Kiricsi and her colleagues at the Department of Biochemistry and Molecular Biology, Faculty of Science and Informatics, for the biochemical measurements and the work on cultured cells;

Dr. Zsolt Rázga and Dr. László Tiszlavicz at the Department of Pathology, Faculty of Medicine, for light and electron microscopic images and their evaluation;

Dr. Gábor Galbács and his colleagues the Department of Inorganic and Analytical Chemistry, Faculty of Science and Informatics, for the ICP-MS measurements.

7. APPENDIX

- I. Horváth T, Papp A, Kiricsi M, Igaz N, Trenka V, Kozma G, Tiszlavicz L, Rázga Zs, Vezér T: Titán-dioxid-nanopálcikák tüdőre kifejtett hatásának állatkísérletes vizsgálata szubakut patkány modellben.
Orvosi Hetilap 160: 57–66 (2019).
- II. Horváth T, Papp A, Igaz N, Kovács D, Kozma G, Trenka V, Tiszlavicz L, Rázga Z, Kónya Z, Kiricsi M, Vezér T: Pulmonary impact of titanium dioxide nanorods: examination of nanorod-exposed rat lungs and human alveolar cells.
International Journal of Nanomedicine 13:7061-7077 (2018).
- III. Horváth T, Vezér T, Kozma G, Papp A: Functional neurotoxicity and tissue metal levels in rats exposed subacutely to titanium dioxide nanoparticles via the airways.
Ideggyógyászati Szemle / Clinical Neuroscience 71:35-42 (2018).
- IV. Horváth T, Papp A, Kovács D, Kálomista I, Kozma G, Vezér T: Electrophysiological alterations and general toxic signs obtained by subacute administration of titanium dioxide nanoparticles to the airways of rats.
Ideggyógyászati Szemle / Clinical Neuroscience 70:127-135 (2017).
- V. Horváth T, Szabó A, Lukács A, Oszlánzi G, Kozma G, Kovács D, Kálomista I, Vezér T, Papp A: Titán-dioxid nanorészecskék szubakut neurotoxicitásának vizsgálata patkány modellben.
Egészségtudomány 60: 7-23 (2016).
- VI. Horváth T, Vezér T, Papp A: Possible Neurotoxicity of Titanium Dioxide Nanoparticles in a Subacute Rat Model.
In: Proceedings of the 21st International Symposium on Analytical and Environmental Problems (Alapi T, Ilisz I, eds.; ISBN:978-963-306-411-5). pp. 368-372 (2015).